Palaeobiodiversity and Palaeoenvironments
https://doi.org/10.1007/s12549-020-00467-8

SENCKENBERG

ORIGINAL PAPER

Palaeoclimate estimates based on the late Miocene to early Pleistocene wood flora of the Bengal Basin: an insight into the climatic evolution of southern Asia

Ruby Ghosh[1] · Anwesha Biswas[2] · Angela A. Bruch[3] · Torsten Utescher[4,5] · Illora Sen[2] · Dipak Kumar Paruya[2] · Anupam Guha[6] · Sultan-Ul-Islam[7] · Subir Bera[2]

Received: 14 April 2020 / Revised: 25 June 2020 / Accepted: 30 September 2020

Abstract

To assess the pattern of climatic evolution during the late Miocene to early Pleistocene in the largest fluvio-deltaic sedimentary system on the Earth, the Bengal Basin (BB), a quantitative palaeoclimatic reconstruction was made, based on 20 fossil wood floras. Those floras show that moisture-loving taxa have decreased considerably since the Miocene, especially at the western margin of the basin. A quantitative reconstruction of climate parameters reveals that the late Miocene–early Pliocene was warmer and wetter than now, yet with spatial variability. Seasonality of temperature was low in the basin and subsequently increased during the late Pliocene–early Pleistocene. Monsoon intensity was weaker during the interval from the late Miocene to early Pleistocene than the present day. A comparison of the retrieved data with some earlier records from sites either influenced by Indian summer monsoon (ISM) or East Asian summer monsoon (EASM) or both, the two branches of the Asian summer monsoon (AM) provide insights into the temporal and spatial patterns of climate evolution in southern Asia during the late Neogene–Quaternary transition. In general, a drop in temperature and a weakening in ISM strength since the early Pleistocene correlate with the global cooling trend, though with spatial differences.

Keywords Late Miocene to early Pleistocene · Climate · Bengal Basin · Fossil woods · ISM · EASM

This article is a contribution to the special issue "Palaeobotanical contributions in honour of Volker Mosbrugger".

Electronic supplementary material The online version of this article (https://doi.org/10.1007/s12549-020-00467-8) contains supplementary material, which is available to authorized users.

✉ Subir Bera
berasubir@yahoo.co.in

[1] Birbal Sahni Institute of Palaeosciences, 53, University Road, Lucknow 226007, India

[2] Centre of Advanced Study, Palaeobotany-Palynology Laboratory, Department of Botany, University of Calcutta, 35, Ballygunge Circular Road, Kolkata 700019, India

[3] ROCEEH Research Centre 'The Role of Culture in Early Expansions of Humans' of the Heidelberg Academy of Sciences, Senckenberg Research Institute and Natural History Museum, 60325 Frankfurt/M, Germany

[4] Senckenberg Research Institute and Natural History Museum, 60325 Frankfurt/M, Germany

[5] Institute for Geosciences, University of Bonn, Nussallee 8, 53115 Bonn, Germany

[6] Department of Botany, Women's College, Agartala, Tripura, India

[7] Department of Geology and Mining, University of Rajshahi, Rajshahi 6205, Bangladesh

Published online: 14 February 2021

Introduction

For a better understanding of possible impacts of global climate change on ecosystems, quantitative climate data beyond the range of instrumental records are crucial (Uhl et al. 2006; Herzschuh et al. 2010), especially the documentation of temporal and spatial climate trends. The late Neogene–Quaternary transition marks the phase when several key tectonic, climatic, and biotic events such as the formation of the Himalaya-Tibetan Plateau, strengthening of the Asian monsoon system, formation of the Antarctic ice sheet and C4 grass expansion (Cerling et al. 1993, 1997; Quade and Cerling 1995; An et al. 2001; Zachos et al. 2001; Zheng et al. 2004; Ségalen et al. 2007; Li et al. 2008) took place simultaneously. When exploring how these tectonic, climatic, and biotic events are linked, and how these factors influenced monsoon history, this phase needs special consideration. An in-depth understanding of monsoonal evolution is crucial as monsoon serves the water requirements of approximately 60% of the world's population and its fluctuations severely affect the agrarian human society and industrial needs, e.g. energy supplies through dams. Basically, a seasonal airflow associated with marked variations in air mass direction, humidity and associated rainfall characterises the monsoon climates (Molnar et al. 2010). Any changes in the monsoon regime may affect vegetation as well as the climate of an area (Lunt et al. 2010). The modern Asian monsoon system consists of two sub-systems, i.e. the Indian summer monsoon (ISM) and East Asian summer monsoon (EASM), and both are characterised by wet summers and dry winters, though different in absolute amounts of precipitation (Wang 2006). ISM influences South Asian countries, while EASM has major influence on the (South)east Asian countries. The evolution of the Asian monsoon (AM) has gained enormous attention for its variability and forcing mechanisms (Kou et al. 2006; Jacques et al. 2011; Yao et al. 2011, 2012; Han et al. 2012; Su et al. 2013; Khan et al. 2014, 2019; Srivastava et al. 2018 etc.). It is crucial to understand to what extent changes in orography and extent of the Himalaya-Tibetan Plateau region, sea–land temperature gradient and associated pressure conditions or interactions between topography and atmospheric-oceanic circulations influenced the Asian monsoon most during the Neogene (Molnar et al. 2010; Wang P. X. et al. 2014; Wang C. S. et al. 2014; Farnsworth et al. 2019; Acosta and Huber 2020; Spicer et al. 2020 and references therein). Further, how changing climate and monsoon history had shaped plant distributions is another open question (Li et al. 2015; Srivastava et al. 2018). To address these issues, a comprehensive comparison between ISM and EASM trends during the late Neogene–Quaternary transition is essential. It is already proved that fossil flora and vegetation may be used as reliable proxies for palaeoclimate reconstructions as they are directly exposed to, and processors of the atmosphere (Khan et al. 2014). Although a large number of quantitative data on Neogene climatic variability are available from Chinese ISM and EASM sites (Kou et al. 2006; Xia et al. 2009; Liu et al. 2011; Yao et al. 2011; Jacques et al. 2011; Qin et al. 2011; Sun et al. 2011; Xing et al. 2012; Su et al. 2013; Huang et al. 2015; Li et al. 2015; Liu and Quan 2016), data from the Indian subcontinent are still far from satisfactory (Tiwari et al. 2012; Khan et al. 2014, 2019; Srivastava et al. 2018). In order to fill this lacuna, we study here 20 fossil wood assemblages from the Bengal Basin (BB).

The BB is one of the least studied peripheral Himalayan foreland basins influenced by the Bay of Bengal (BOB) branch of ISM. It was formed due to the collision of the Indian and Eurasian plate and preserves palaeoenvironmental records dating back to the late Mesozoic (Alam 1989; Roy and Roser 2013). Interestingly, the BB records a large number of fossil woods which helped to explore the vegetation and climate of this region during the Neogene (Chowdhury and Tandon 1952; Ghosh and Taneja 1961; Ghosh and Kazmi 1961; Deb and Ghosh 1974; Ghosh and Roy 1978, 1979a, b, c, d, 1980, 1981, 1982; Roy and Ghosh 1979, 1980; Bande and Prakash 1980, Bande and Srivastava 1989; Acharya and Roy 1986, Agarwal et al. 1989; Bera and Banerjee 1990, 1997, 2001, Bera et al. 2000; Awasthi et al. 1994, 2000; Poole and Davies 2001, Sen et al. 2004, 2012; Mehrotra and Bhattacharyya 2002; Mehrotra et al. 2006, 2017; Sen and Bera 2005; Biswas et al. 2019). Fossil woods, especially selected features of dicotyledonous wood, have ecologic and/or phylogenetic significance such as the presence/absence of growth rings, mean tangential diameter of vessel lumina, vessel frequencies, vessel grouping, perforation plate, porosity, intervessel pits, paratracheal and apotracheal axial parenchyma and rays cellular composition. All these and other characters have been found to vary over geologic time and in response to climatic changes (Wheeler and Baas 1991, 1993; Baas and Wheeler 2011). For example, the presence of growth rings is related to seasonality (however, sometimes may also be due to switching of resources to and from reproduction), the width of the ring may vary with favourability of growing conditions, variations in ring width may be related to year-to-year climate variance, and diameter and density of vessels are often used to infer presence of tropical vs. temperate climatic conditions (Creber and Chaloner 1984; Francis 1984; Thayn et al. 1985; Parrish and Spicer 1988; Wheeler and Baas 1991; Ash and Creber 1992). Similarly, vessel diameter and density, perforation plate, and pit membrane porosity regulate the hydraulic conductivity of the plant body (Baas and Wheeler 2011). In flowering plants, bordered pits are used to play an important role in permitting water flow among adjacent tracheary elements. Variations in their structure are often associated to balancing the conflict between hydraulic efficiency (conductivity) and safety from air entry at the pit membrane (air seeding). For instance, the vestured pits (a kind of bordered pits) are mostly minute and

simple in woody plants from cold and boreal environments, while those in the plants from mesic and dry sub-tropical lowlands show a distinctly developed branched network (Jansen et al. 2004). Thus, considering the significance of the wood fossils in vegetation and climate reconstructions, we apply the Coexistence Approach (CA) on the BB wood assemblages to unravel the climatic history during the late Miocene to early Pleistocene and associated vegetation changes. We compare the quantitative climate data from the BB to datasets from 31 other sites influenced by either ISM or EASM from India and southern/eastern China. This will help to explore whether the temporal and spatial trends of climate variability in this part of Asia, during the late Miocene to early Pleistocene, were synchronous or asynchronous and to investigate possible underlying forcing mechanisms.

Study area: geological setting, modern vegetation and climate

The Bengal Basin (BB), covering an extensive area including Bangladesh and some eastern provinces of India (West Bengal, Meghalaya, Mikir Hills, Assam, Nagaland, Cachar and Surma Valley and Tripura), is one of the largest sedimentary basins of the world (Banerji 1984; Roybarman 1992). Throughout the period of its evolution beginning in the Cretaceous, the BB has undergone several phases of transgression and regression, periodic uplifts and local subsidence (Lindsay et al. 1991; Mukherjee et al. 2009). The greater Bengal Basin is bounded by the Indo-Burma Ranges to the east, exposures of the Indian craton to the west, the Shillong Plateau to the north and southward by the Bay of Bengal (Gani and Alam 2003).

The BB is well known for the development of one of the thickest (about 20 km) sedimentary successions in the world, represented by a series of genetically related, but widely spaced, geological provinces. During its evolution, the BB has undergone two successive developmental phases such as (i) a marine transgressive phase (with minor regressions), which lasted until the end of the Eocene, and (ii) a regressive phase with an intermediate transgressive stage, that led to a series of continental, fluvio-deltaic to marginal marine sediments during the Oligo–Miocene. Post Eocene sedimentation was complex, and influenced by several tectonic events that periodically affected its configuration and surrounding regions (Banerji 1984).

Bangladesh occupies the largest part of the BB (Salt et al. 1986). Two major tectonic sub-units of this part of the BB are: a geosynclinal basin in the southeast and a stable Precambrian Platform in the northwest. The huge thickness of this geosynclinal basin is characterised by clastic sedimentary rocks, sandstones and shales. This sedimentary succession is mostly Paleogene to Neogene in age, with the Surma Group (Miocene) separated from the Barail Group (Oligocene) by an unconformity. The Surma Group is sub-divided into two formations, i.e. a lower sandy Bhuban Formation and an upper argillaceous Boka Bil Formation. The Tipam Group (late Miocene to Pliocene) overlaying the Surma Group is subdivided into the Tipam Sandstone formation and Girujan Clay formation, followed by the Dupi Tila formation (Pliocene–Pleistocene). The Tipam Sandstone Formation is mainly composed of medium-grained sandstones, frequently cross-bedded, with little shale and wood fragments, deposited under fluvial conditions. The Girujan Clay Formation on the other hand is a shale unit and formed within a lacustrine environment. The Dupi Tila Formation is composed of medium to coarse, loosely compacted cross-bedded sandstone, occasionally pebbly, indicating deposition in a river environment. Lignite and fragments of petrified woods are frequently present in the lower part of Dupi Tila Formation in the eastern and southern Surma Basin, the Chittagong Hill Tracts and the Tripura Fold Belt (Poole and Davies 2001; Sen et al. 2004). A generalised Cenozoic stratigraphic division of the Bengal Basin (following Uddin and Lundberg 1998; Uddin et al. 2007) is presented in Table 1.

In the eastern part of BB, the Neogene sediments of the Indian state of Tripura have been classified into Boka Bil formation of the Surma Group, the Tipam Group and Dupi Tila Group (Roy 1968-69). At the western margin of the BB, the geology of the fossil-bearing Neogene sediments has been studied by Hunday (1954) in detail. These exposures consist of yellowish ferruginous sandstones and red shales, associated with quartz and gravel beds underlain by clay, and are comparable to the Tipam Sandstone by age. These beds are rich in dicotyledonous fossil woods. Earlier works (Hunday 1954; Hunday and Banerjee 1967; Ghosh and Roy 1979a, b, c, d, 1980; Bande and Prakash 1980) assign a Mio–Pliocene age to these sediments, equivalent to the Tipam Series.

The modern climate of the BB is typically tropical, with high rainfall and moderate seasonality of temperature. The entire basin is influenced by the Bay of Bengal (BoB) branch of the ISM, where maximum rainfall occurs between June–July–August–September (JJAS) and winter months receive the least rainfall. A west to east increasing rainfall gradient is observed in the basin where the western margin of the basin receives less rainfall than its eastern part, due to orographic effects of the Chotanagpur Plateau in the west. The presence of the Himalaya in the north also has a considerable impact on the climatic conditions of the basin. The Himalayan range prevents the monsoon winds from BoB to cross over to the north, leading to heavy rainfall in the northern BB. Three specific seasons are recognised in the climatic calendar of the basin, i.e. a hot-dry (February–March–April–May; FMAM), hot-wet (JJAS) and a cooler period (October–November–December–January; ONDJ) (Chatterjee 1970). Mean annual temperature of the basin varies between c. 8 and 31 °C.

Table 1 A generalized Cenozoic stratigraphy of the Bengal Basin (after Uddin and Lundberg 1998; Uddin et al. 2007)

Age	Unit		Lithology
Pliocene to Pleistocene	Dupi Tila Sandstone		Medium to coarse-grained, massive to cross-bedded, variously coloured sand(stone) with pebbles, clay galls with coal and wood fragments
Late Miocene to Pliocene	Tipam Group	Girujan Clay	Brown to blue mottled clay with calcareous nodules
		Tipam Sandstone	Yellow-brown to orange, medium to coarse grained, massive and cross-bedded, sand(stone) with pebbles and coal and wood fragments.
Unconformity			
Middle to late Miocene	Surma Group	Boka Bil Formation	Alternation of bedded and rippled mudstone, siltstone and sandstone with calcareous concretions; top is marked by the 'upper marine shale'
Early to Middle Miocene		Bhuban Formation	Light grey to light yellow, bedded siltstone, sandstone and sandy mud in top unit; blue to yellowish grey silty and sandy mudstone in the middle unit; bedded siltstone, sandstone and sandy mud in the lower unit
Unconformity			
Oligocene	Barail Formation		Pink, massive, medium-to coarse-grained sand(stone)
Late Eocene	Kopili Formation		Thinly bedded, fossiliferous mudstone
Middle Eocene	Sylhet Limestone		Nummulitic limestone

Forests of the Bangladesh part of the BB are divided into three zones, i.e. (i) Chittagong Hill Tracts in the southeast, (ii) Madhupur Tracts in Central Bangladesh, and (iii) Sunderbans in the south (Reimann 1993). The hilly tract of Chittagong hosts two varieties of forests, the tropical evergreen forest characterised by taxa like *Artocarpus*, *Tetrameles*, *Hopea*, *Sterculia*, *Mesua*, *Cedrella* and *Bursera*, and the tropical mixed evergreen forest comprising of *Dipterocarpus*, *Lophopetalum*, *Dillenia*, *Mirabilis* and *Terminalia*. The tropical moist deciduous forests of the Madhupur Tract of Central Bangladesh are composed mainly of *Shorea robusta*, *Butea monosperma*, *Adina cordifolia*, *Albizia* spp., *Litsea monopetala*, *Grewia microcos*, *Sterculia villosa*, *Lagerstroemia parviflora*, and *Terminalia* spp. The Sunderbans comprise littoral and swampy forests (dominated by *Avicennia*, *Aegiceras*, *Bruguiera*, *Ceriops*, *Exoecaria*, *Kandelia*, *Phoenix* spp., *Nypa fruticans*, *Sonneratia*, and *Xylocarpus*) in the deltaic part of the basin.

In the Indian part of the BB, four distinct vegetation zones occur (Champion and Seth 1968) such as (i) tropical dry deciduous forests, (ii) tropical moist deciduous forests, (iii) tropical moist semi-evergreen forests scattered in patches, and (iv) littoral and swampy forests in the deltaic part of the basin, i.e. the Sunderbans. The westernmost part of the BB is mostly covered by tropical dry deciduous forests. Those are dominated by *Acacia*, *Aegle*, *Anogeissus latifolia*, *Bauhinia Buchanania*, *Butea*, *Diospyros*, *Grewia*, *Hardwickia*, *Madhuca*, *Phyllanthus*, *Pterospermum*, *Semecarpus*, *Shorea*, *Tectona*, *Terminalia*, and *Zizyphus*. Tropical moist deciduous forests cover the central part of the western margin of the BB. They show a similar floristic composition to those of the Madhupur Tract of Central Bangladesh. The Himalayan foothill region at the northern and eastern margins of the BB is covered by tropical moist semi-evergreen and moist deciduous forests. While they are dominated by *Adina cordifolia*, *Albizia*, *Bambusa*, *Artocarpus hirsuta*, *Bauhinia variegata*, *Calamus*, *Dalbergia latifolia*, *Dalbergia sissoo*, *Dipterocarpus*, *Duabanga*, *Eugenia* sp., *Garcinia*, *Hopea parviflora*, *Lagerstroemia*, *Litsea*, *Mallotus*, *Mangifera indica*, *Mesua ferrea*, *Mitragyna parviflora*, *Sterculia*, *Tectona grandis*, *Terminalia bellerica*, *Terminalia tomentosa*, *Terminalia paniculata*, *Shorea robusta*, and *Syzygium cumini*, and *Terminalia* spp. *Tectona grandis* and *Shorea* both can grow in the tropical dry deciduous as well as in the tropical moist deciduous forests.

Materials and methods

In order to study the vegetation and climate during the late Miocene to early Pleistocene of the BB, about 129 well preserved silicified wood specimens were examined from across the basin (Table S1). At the western margin of the BB, samples come from different locations of the Birbhum district (Ulpahari, Muhammad Bazar, Labpur, Uttar Raipur, Muluk, Bolpur and Santiniketan), West Bengal, belonging to the Tipam Group of late Miocene–Pliocene age (Fig. 1; Table 2). Samples procured from different locations of Tripura (Khowai, Udaipur, Melaghar, Manu Bazar, Bishalgarh, Laljuri, and Amarpur) also belong to the Tipam Group (late Miocene–Pliocene) (Fig. 1; Table 2). Wood specimens collected from the Comilla district of Bangladesh belong to the Dupi Tila Formation of Pliocene –Pleistocene age (Fig. 1; Table 2). The wood dataset is combined to eight assemblages, considering their geologic age and geographic occurrence in the basin, in order to explore whether the environmental evolution in this wide basin was synchronous or asynchronous (Table 3).Seven assemblages are of late Miocene–Pliocene age while the Lalmai Hill, Comilla, and

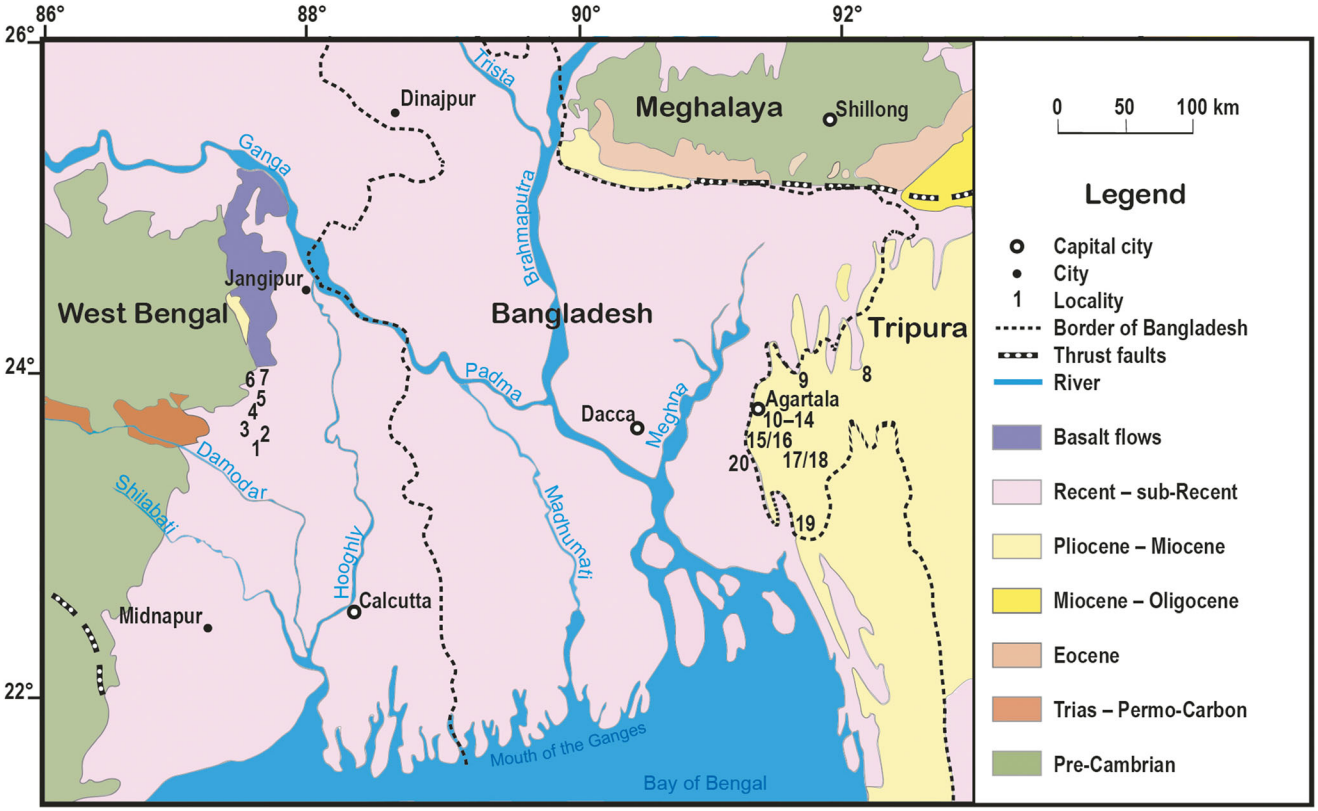

Fig. 1 Geological map of the Bengal Basin with fossil wood localities. *1* Bolpur; *2* Muluk; *3* Santiniketan; *4* Uttar Raipur; *5* Labpur; *6* Ulpahari; *7* Muhammad Bazar; *8* Laljuri; *9* Khowai; *10* Teliamura; *11* Kunjaban; *12* Agartala; *13* Yogendranagar; *14* Baramura; *15* Melaghar; *16* Bishalgarh; *17* Amarpur; *18* Udaipur; *19* Manu Bazar; *20* Lalmai Hill (modified after Bera and Banerjee 2001)

Bangladesh assemblages have a Pliocene-Pleistocene age (Table 3).

Preparation of fossil woods

To study anatomical details, all collected silicified woods were sectioned transversally and longitudinally (radially and tangentially), and permanent slides were prepared using the standard method by Hass and Rowe (1999). The wood sections were then fixed to glass slides and polished with different grades of carborundum powder and mounted in Canada balsam (Lacey 1963). The following anatomical characters of the fossil woods, which provide information on overall environmental conditions, were described and measured, i.e. presence/absence of growth rings, mean tangential diameter of vessel lumina, vessel frequencies, vessel grouping, perforation plate, porosity, intervessel pits, paratracheal and apotracheal axial parenchyma, and rays cellular composition.

Identification of fossil woods

The studied fossil wood taxa were also assigned to their Nearest Living Relatives (NLRs). When dealing with fossil woods, the NLR approach is frequently used to infer palaeoclimatic information, based on the assumption that very little or insignificant change has taken place in the relation of wood characters to climate (Prakash et al. 1994; Estrada-Ruiz et al. 2007; Jeong et al. 2009; Feng et al. 2010; Bamford 2011; Mehrotra et al. 2011; Tiwari et al. 2012). The identification of NLRs of the silicified woods was done by comparing the materials with the database kept in the Xylarium of the Forest Research Institute, Dehradun and Palaeobotany-Palynology Laboratory, University of Calcutta, and published records (Metcalfe and Chalk 1950, 1987; Cutler and Gregory 1998; Inside wood at http://insidewood.lib.ncsu.edu/search). Lists of the studied fossil wood taxa, their NLRs, and anatomical characters are presented in Tables S1–S3. All xylotomical slides are kept in the repository of Palaeobotany-Palynology Laboratory, University of Calcutta. The anatomical terminologies used for the description of woods are after Wheeler et al. (1986) and International Association of Wood Anatomists (IAWA 1989).

Estimation of Carlquist's vulnerability and mesomorphy indices

To determine the susceptibility or vulnerability of woods to water stress condition, Wolfe and Upchurch (1987) used Carlquist's vulnerability index (V). By using the same principle here we measure the vulnerability index (V), with $V =$ mean vessel diameter/mean number of vessels per mm^2 of

Table 2 List of localities with fossil wood taxa used for climate analyses

Site no.	Assemblage	Locality	Coordinates	Formation	Age	No. of taxa	References
1	Bolpur	Birbhum District, West Bengal, India	N 23.6369° E 87.6469°	Equivalent to Tipam Formation	Late Miocene/Pliocene	5	Ghosh and Roy (1981)
2	Muluk	Birbhum District, West Bengal, India	N 23.6542° E 87.7203°	Equivalent to Tipam Formation	Late Miocene/Pliocene	4	Unpublished
3	Santiniketan	Birbhum District, West Bengal, India	N 23.7000° E 87.6833°	Equivalent to Tipam Formation	Late Miocene/Pliocene	12	Deb and Ghosh (1974); Ghosh and Roy (1979b , d); Roy and Ghosh (1979); Bande and Prakash (1980)
4	Uttar Raipur	Birbhum District, West Bengal, India	N 23.7833° E 87.7500°	Equivalent to Tipam Formation	Late Miocene/Pliocene	7	Bera and Banerjee (2001)
5	Labpur	Birbhum District, West Bengal, India	N 23.8167° E 87.8006°	Equivalent to Tipam Formation	Late Miocene/Pliocene	8	Ghosh and Roy (1979a , c); Ghosh and Roy (1982); Roy and Ghosh (1980)
6	Ulpahari	Birbhum District, West Bengal, India	N 23.9501° E 87.6666	Equivalent to Tipam Formation	Late Miocene/Pliocene	14	Unpublished
7	Muhammad Bazar	Birbhum District, West Bengal, India	N 24.0000° E 87.7500°	Equivalent to Tipam Formation	Late Miocene/Pliocene	6	Bande and Srivastava (1989); Bera and Banerjee (2001)
8	Laljuri	Unakoti District, Tripura, India	N 24.1038° E 91.9447°	Tipam Group	Late Miocene/Pliocene	5	Mehrotra et al. (2017)
9	Khowai	Khowai District, Tripura, India	N 24.0672° E 91.6057°	Tipam Sandstone Formation	Late Miocene/Pliocene	2	Thesis of Sen (2006) (unpublished)
10	Teliamura	Khowai District, Tripura, India	N 23.8411° E 91.6277°	Tipam Sandstone Formation	Late Miocene/Pliocene	12	Ghosh and Taneja (1961); Ghosh and Kazmi (1961); Acharya and Roy (1986); Mehrotra et al. (2006)
11	Kunjaban	West Tripura District, Tripura, India	N 23.8635° E 91.2903°	Tipam Sandstone Formation	Late Miocene/Pliocene	11	Sen and Bera (2005) and Thesis of Sen (2006) (unpublished)
12	Agartala	West Tripura District, Tripura, India	N 23.8315° E 91.2868°	Tipam Sandstone Formation	Late Miocene/Pliocene	5	Thesis of Sen (2006) (unpublished)
13	Yogendranagar	West Tripura District, Tripura, India	N 23.8114° E 91.3036	Tipam Sandstone Formation	Late Miocene/Pliocene	6	Sen and Bera (2005) and Thesis of Sen (2006) (unpublished)
14	Baramura	West Tripura District, Tripura, India	N 23.8158° E 91.58°	Tipam Sandstone Formation	Late Miocene/Pliocene	11	Sen and Bera (2005) and Thesis of Sen (2006) (unpublished)
15	Melaghar	Sipahijala District, Tripura, India	N 23.4973° E 91.3313°	Tipam Sandstone Formation	Late Miocene/Pliocene	7	Thesis of Sen (2006) (unpublished)
16	Bishalgarh	Sepahijala District, Tripura, India	N 23.6767° E 91.2731°	Tipam Group	Late Miocene/Pliocene	1	Mehrotra and Bhattacharyya (2002)
17	Amarpur	Gomati District, Tripura, India	N 23.5300° E 91.6344°	Tipam Sandstone Formation	Late Miocene/Pliocene	1	Awasthi et al. (1994)
18	Udaipur	Gomati District, Tripura, India	N 23.5333° E 91.5000°	Tipam Group	Late Miocene/Pliocene	1	Mehrotra et al. (2006)
19	Manu Bazar	South Tripura District, Tripura, India	N 23.0667° E 91.6167	Tipam Group	Late Miocene/Pliocene	2	Mehrotra et al. (2006)
20	Lalmai Hill	Lalmai Hill Range, Comilla District, Bangladesh	N 23.4278° E 91.1333°	Dupi Tila Formation	Plio-Pleistocene	9	Sen et al. (2012)

Table 3 Climate estimates for the major fossil wood assemblages, arranged by geological time and geographic region

Analysis unit	Combined assemblages	Age	No. of taxa	No. of climate data
Ulpahari assemblage	Birbhum District, West Bengal, India	Late Miocene/Pliocene	14	10
(A) North Birbhum District assemblage	Muhammad Bazar/Ulpahari, Birbhum District, West Bengal, India	Late Miocene/Pliocene	17	12
(B) Central Birbhum District assemblage	Uttar Raipur/Labpur, Birbhum District, West Bengal, India	Late Miocene/Pliocene	14	12
(C) South Birbhum District assemblage	Bolpur/Muluk/Santiniketan, Birbhum District, West Bengal, India	Late Miocene/Pliocene	18	15
(D) Khowai District assemblage	Khowai/Teliamura, Khowai District, Tripura, India	Late Miocene/Pliocene	14	10
(E) West Tripura District assemblage	Agartala/Baramura/Kunjaban/Yogendrangar, West Tripura District, Tripura, India	Late Miocene/Pliocene	21	14
(F) Tripura assemblage	All localities of Tripura, India	Late Miocene/Pliocene	45	22
(G) Lalmai Hill assemblage	Lalmai Hill Range, Comilla District, Bangladesh	Plio-Pleistocene	9	8

Analysis unit	MAT (°C) Coexistence intervals (CI) and bordering taxa	MAP (mm)	CMT (°C)
Ulpahari assemblage	24.1–27.7 (*Anisoptera–Anisoptera*)	1682–3141 (*Chisocheton–Anisoptera*)	19.4–26.1 (*Anisoptera–Ormosia*)
(A) North Birbhum District assemblage	24.1–27.7 (*Anisoptera–Anisoptera*)	1682–3141 (*Chisocheton–Anisoptera*)	19.4–26.1 (*Anisoptera–Ormosia*)
(B) Central Birbhum District assemblage	23.3–26.6 *(Lannea–Lannea)*	1682–3151 (*Chisocheton–Albizia*)	17.8–25.6 (*Lannea–Lannea*)
(C) South Birbhum District assemblage	24.1–27.2 *(Anisoptera–Diospyros)*	1748–3141 (*Koompassia–Anisoptera*)	20.6–26.1 (*Koompassia–Diospyros*)
(D) Khowai District assemblage	26.1–27.7 (*Bouea–Afzelia–Intsia*)	1650–3151 (*Bouea–Cassia*)	22.2–27 (*Bouea–Cassia*)
(E) West Tripura District assemblage	26.5–27.6 (*Gonystylus–Afzelia–Intsia)*	1930–3141 (*Gonystylus–Anisoptera*)	25–27 (*Gonystylus–Albizzia*)
(F) Tripura assemblage	26.5–27.6 *Gonystylus–Afzelia–Intsia)*	1930–3141 (*Gonystylus–Anisoptera*)	25–27 (*Gonystylus–Albizzia*)
(G) Lalmai Hill assemblage	26.5–27.5 (*Kingiodendron–Careya*)	2099–3141 (*Kingiodendron–Anisoptera*)	25–25.6 (*Kingiodendron–Careya*)

Analysis unit	WMT (°C) Coexistence intervals (CI) and bordering taxa	MPwet (mm)	MPdry (mm)	MPwarm (mm)
Ulpahari assemblage	27.2–28.9 (*Anisoptera–Milletia*)	343–389 (*Chisocheton–Cynometra*)	11–109 (*Chisocheton–Ormosia*)	128–227 (*Cynometra–Cynometra*)
(A) North Birbhum District assemblage	27.2–28.9 (*Anisoptera–Milletia*)	343–389 (*Chisocheton–*Arecaceae)	11–109 (*Chisocheton–Ormosia*)	128–227 (*Cynometra–Arecaceae*)
(B) Central Birbhum District assemblage	26.7–28.1 (*Lannea–Cassia*)	343–389 (*Chisocheton–Cassia*)	11–25 (*Chisocheton–Lannea*)	128–206 (*Cynometra–Lannea*)
(C) South Birbhum District assemblage	27.2–28.1 (*Anisoptera–Cassia)*	270–389 (*Gluta–Arecaceae*)	46–155 (*Koompassia–Mangifera*)	128–221 (*Cynometra–Cassia*)
(D) Khowai District assemblage	27.5–28.1 (*Palaquium–Cassia*)	300–389 (*Palaquium–Cassia*)	11–165 (*Palaquium–Afzelia/Intsia*)	163–221 (*Palaquium–Cassia*)
(E) West Tripura District assemblage	27.7–28.1 (*Gonystylus–Gonystylus*)	270–389 (*Gluta–Sonneratia*)	103–155 (*Gonystylus–Mangifera*)	135–221 (*Gonystylus–Gluta*)
(F) Tripura assemblage	27.7–28.1 (*Gonystylus–Cassia*)	300–389 (*Palaquium–Cassia*)	103–155 (*Gonystylus–Mangifera*)	135–221 (*Palaquium–Cassia*)
(G) Lalmai Hill assemblage	28.3–28.9 (*Careya–Milletia*)	343–389 (*Chisocheton–Cynometra*)	11–56 (*Chisocheton–Careya*)	128–146 (*Cynometra–Careya*)

fossil woods (Carlquist 1977). Similarly, the mesomorphy (M) of the fossil wood was calculated by multiplying the 'vulnerability index' with the mean vessel element length (Carlquist 1977). A taxon is considered xeromorphic, i.e. adapted to xeric conditions, if the 'V' value remains < 1, while a value > 3 suggests that a taxon is adapted to a humid environment where soil available water is plenty (mesomorphy). However, 'M' values < 30 indicate true xeromorphy and values c. 200 or higher suggest mesomorphy (Carlquist 1977).

Climate analysis

In the past few decades, rapid development in methods of quantitative palaeoclimate reconstructions using plant fossils has afforded means of comparing the past variability in climate parameters (Liu et al. 2011). Among those methods, the Coexistence Approach (CA) (Mosbrugger and Utescher 1997; Utescher et al. 2014) is being used widely in Neogene climate reconstructions, due to its independence of the fossil plant organs studied. This method assumes that climatic requirements of fossil taxa are similar to those of their NLRs. By considering the climatic requirements of the NLRs, the CA finds the climatic range in which the maximum number of NLRs of a given fossil assemblage can coexist. This is also known as the 'coexistence interval' (CI) which is calculated separately for every climate parameter studied, and is believed to be the best estimate of the palaeoclimatic conditions under which the fossil flora once lived. The computer program CLIMSTAT (a noncommercial java application available via www.neclime.de) facilitates the application of the CA. All technical details on the method are given in Utescher et al. (2014) and on the NECLIME website (www.neclime.de). The climatic requirements of the NLRs are obtained from the PALAEOFLORA database (Utescher and Mosbrugger 2015), and all data used here are given as supplementary material (Table S4). Seven climatic parameters are considered in this study, i.e. mean annual temperature (MAT), temperature of the coldest month (CMT), temperature of the warmest month (WMT), mean annual precipitation (MAP), wettest month precipitation (MPwet), driest month precipitation (MPdry) and warmest month precipitation (MPwarm). From the difference between summer and winter temperatures, the mean annual ranges of temperature is calculated, i.e. mean annual range of temperature (MART = WMT − CMT). Similarly, the difference between wettest and driest months precipitation is considered the mean annual range of precipitation (MARP = MPwet − MPdry).

We also calculated a monsoon intensity index (MSI), based on the precipitation variables. To assess monsoon intensity, various monsoon indices were defined (Liu and Yin 2002; van Dam 2006; Xu et al. 2008; Liu et al. 2011; Xing et al. 2012; Jacques et al. 2013; Li et al. 2015). In order to compare our data with other fossil localities, we used a modified MSI equation. We substituted GSP with MAP in our study as in Li et al. (2015), and used MPwet and MPdry instead of MPQwet/MPQdry. Thus, the monsoon index we use here is as follows:

$$MSI = (MPwet - MPdry)/MAP*100.$$

With an increasing number of taxa in the analysis the resolution and reliability of the resulting CIs increase. So, assemblages with ten or more taxa for which climate parameters are known are best suited for the analysis (Mosbrugger and Utescher 1997). Though, the Lalmai Hill assemblage provides only eight taxa with climate data, but is nevertheless considered as it represents the only plant assemblage of Pliocene –Pleistocene age from the BB.

Furthermore, we compare the data obtained from the BB xylofloras with published quantitative palaeoclimate records from 31 localities in southern Asia, which depict the climate evolution during the late Miocene to early Pleistocene (Tables S5 and S6). The sites selected are either influenced by ISM or EASM which will help to understand whether the evolution of these two branches of ASM were synchronous or asynchronous.

Results

A total number of 129 silicified wood specimens from 20 localities, identified to 80 different species under 45 genera and 20 families are considered in this study. All the recovered silicified woods of the BB are diffused porous with indistinct growth rings, with large to medium-sized vessels with uniform diameter (Figs. S1–S3). The simple perforation plate feature is found to be exclusive in the BB woods (Tables S2 and S3; Figs. S1–S3). Among the different types of intervessel pits, the alternate type (81.25–100%) is most common. Similarly, different types of paratracheal parenchyma such as scanty, vasicentric, aliform, and confluent types are abundant in different woods of the BB. Septate fibres are less abundant than the non-septate fibres. Ray cells are found comprising mostly of procumbent cells (25–46.15%) (Tables S2 and S3). To measure the susceptibility or vulnerability of woods to water stress or drought conditions, Wolfe and Upchurch (1987) used Carlquist's (1977) vulnerability index (V). The BB fossil woods show high 'V' values in most of the cases (Table S3).

The dataset is split into seven assemblages such as A. North Birbhum District, B. Central Birbhum District, C. South Birbhum District, D. Khowai District, E. West Tripura District, F. Tripura, and G. Lalmai Hill assemblage (Table 3) to understand the spatial and temporal patterns in vegetation and climate. Considering the NLRs of the fossil taxa, the abundance of different forest elements in the assemblages is determined and represented in Fig. 2. The

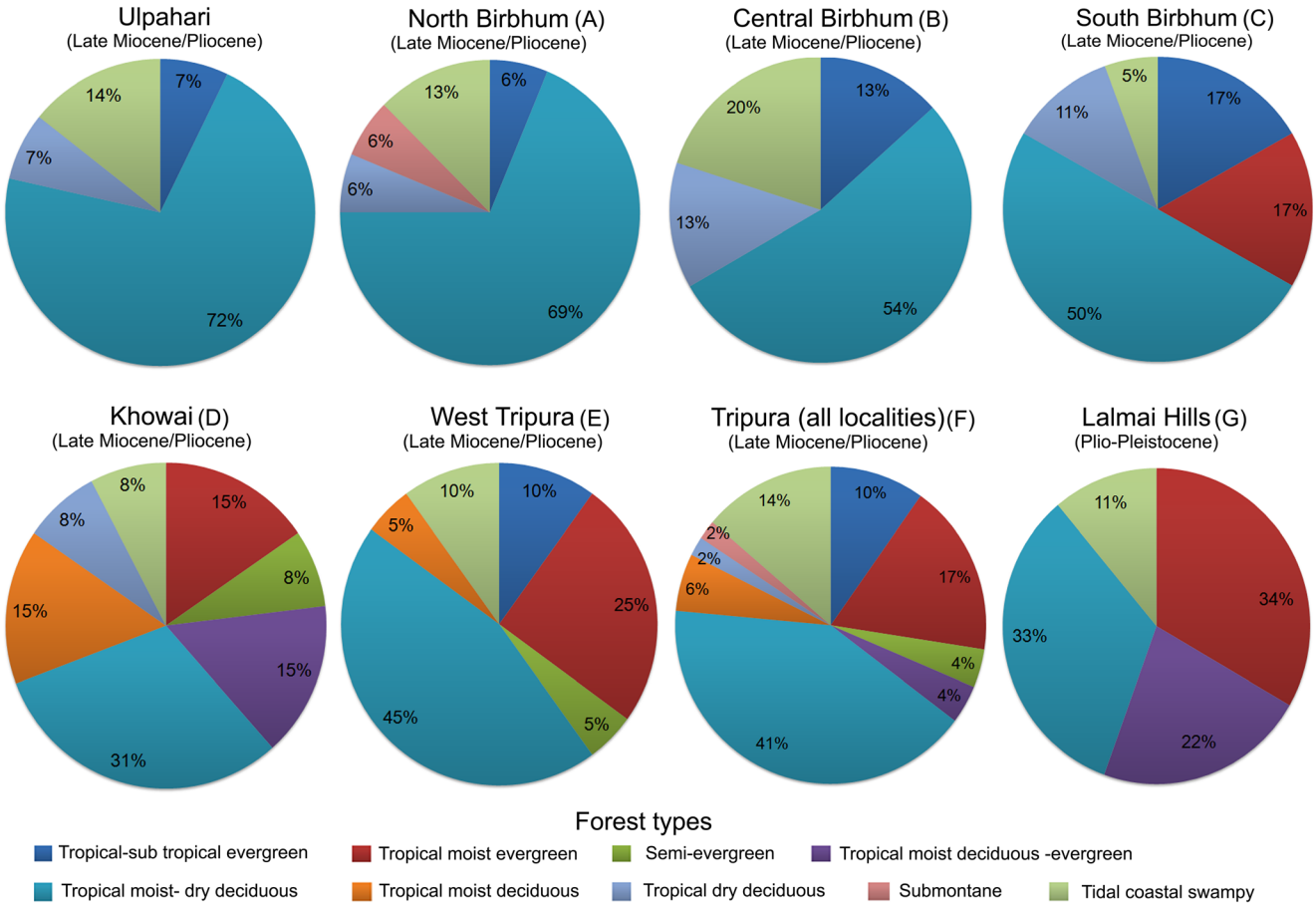

Fig. 2 Late Miocene to early Pleistocene floristic pattern of the Bengal Basin connected to major forest elements

quantitative climate data for all assemblages are visualized in Figs. 3 and 4 and given in Table 3 where the species that represent the limits of the coexistence intervals are also mentioned.

Western margin of the BB

North Birbhum District assemblage (A)

The Ulpahari and Muhammad Bazar wood assemblages are combined into the North Birbhum District assemblage, which comprises of 17 taxa under seven angiosperm families and are late Miocene–early Pliocene in age (Tables 1, 2 and 3). Of these wood taxa, the Ulpahari wood assemblage consists of 14 taxa (Tables 2 and 3). To assess if the combined wood assemblage differs in CA reconstructed climatic parameters from those of any assemblage with a sufficient number of taxa from the same region, both the Ulpahari and North Birbhum assemblages are represented in Tables 2 and 3 and Figs. 1, 2, 3, and 4 as examples. The NLRs of the Ulpahari fossil wood taxa indicate that during this time the forest was dominated by members of Fabaceae (such as *Albizia*, *Cynometra*, *Millettia*, and *Ormosia*) and Dipterocapaceae (such as *Anisoptera*, *Dipterocarpus*, and *Shorea*), associated with Anacardiaceae (*Mangifera*), Meliaceae (*Chisocheton)*, and Combretaceae (*Terminalia*). The floristic analysis suggests that a tropical deciduous forest (72%) prevailed in this area. As most of its elements occur in moist forests as well as in dry ones, no distinction between tropical moist deciduous and tropical dry deciduous forests can be made here. Besides these, some tidal coastal swampy forest elements (14%) like *Cynometra polyandra* and *Cynometra ramiflora* were also present in the assemblage (Fig. 2). 'V' values of these fossil woods vary between 6.3 and 26.1, while 'M' values remain > 200 for all (Table S5). The combined North Birbhum wood assemblage also confirms the fact that in the late Miocene–early Pliocene, there was a tropical deciduous forest in this region. However, the combined assemblage shows a minor variation in abundances of forest elements, which may be due to low taxon diversity in the Muhammad Bazar assemblage. In the combined assemblage deciduous elements (69%) are followed by tidal coastal swampy (13%), tropical dry deciduous (6%) and tropical–subtropical evergreen (6%) forest elements. In addition, the submontane element *Kayea assamica* (Clusiaceae) is also observed in this assemblage (Fig. 2). For both the cases, the coexistence intervals (CIs) show similar results suggesting

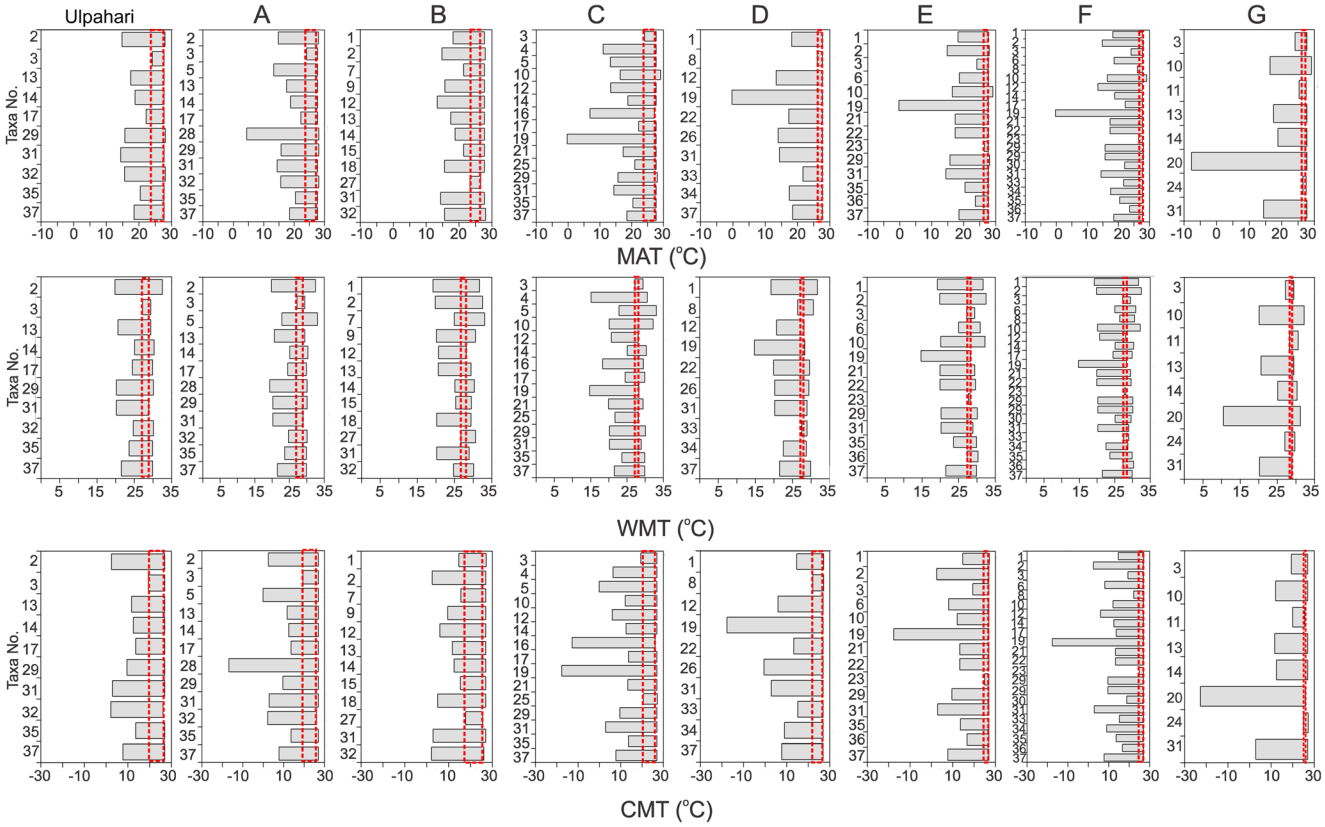

Fig. 3 The coexistence intervals of temperature parameters (MAT, WMT, and CMT) of the fossil wood assemblages (vertical red lines indicate common range for all the NLRs)

that combined wood assemblages are equally efficient in capturing climate signals as any single assemblage with a sufficient number of taxa for CA. CIs for MAT, MAP, WMT, CMT, MPwet, MPdry, and MPwarm for both assemblages range between 24.1–27.7 °C, 1682–3141 mm, 27.2–28.9 °C, 19.4–26.1 °C, 343–389 mm, 11–109 mm and 128–227 mm respectively (Table 3; Figs. 3 and 4).

Central Birbhum District assemblage (B)

In the Central Birbhum District assemblage 14 wood taxa from Labpur and Uttar Raipur (late Miocene−early Pliocene) are combined (Table 3). The dominant families are Fabaceae (different species of *Albizia*, *Cassia*, *Dialium*, *Millettia*, *Ormosia*, and *Pahudia*), Anacardiaceae, Meliaceae, and Arecaceae. Here, also moist to dry deciduous elements (69%) are found to be most abundant followed by tropical dry deciduous (13%), tidal coastal swampy (13%), and tropical-subtropical evergreen (13%) elements (Fig. 2).

The reconstructed CIs for this wood assemblage range between 23.3–26.6 °C for MAT, 26.7–28.1 °C for WMT, 17.8–25.6 °C for CMT, 1682–3151 mm for MAP, 343–389 mm for MPwet, 11–25 mm for MPdry, and 128–206 mm for MPwarm (Table 3; Figs. 3 and 4).

South Birbhum District assemblage (C)

Wood taxa recovered from the Muluk, Bolpur, and Santiniketan assemblages are combined within this assemblage (Table 3), which consists of 18 taxa from 10 families. Members of the Dipterocarpaceae (23%), Fabaceae (23%), and Combretaceae (12%), along with families like Anacardiaceae, Clusiaceae, Burseraceae, and Arecaceae characterise this late Miocene−Pliocene wood assemblage. This assemblage also includes families which are not observed in the earlier three assemblages such as Burseraceae (*Canarium*), Ebenaceae (*Diospyros*), Euphorbiaceae (*Mallotus/Blumeodendron/Trewia/Cleidion*), and Araucariaceae (*Araucaria/Agathis*). Palaeofloristic analysis reveals dominance of tropical moist to dry deciduous forest elements (50%), followed by tropical sub-tropical evergreen (17%), tropical dry deciduous (11%), and tidal coastal swampy (5%) elements. Representatives of tropical moist evergreen forests (17%) are also recorded from this part of the BB (Fig. 2).

For this wood assemblage, CIs indicate 24.1–27.2 °C for MAT, 27.2–28.1 °C for WMT, 20.6–26.1 °C for CMT, 1748–3141 mm for MAP, 270–389 mm for MPwet, 46–155 mm for MPdry, and 128–221 mm for MPwarm (Table 3; Figs. 3 and 4).

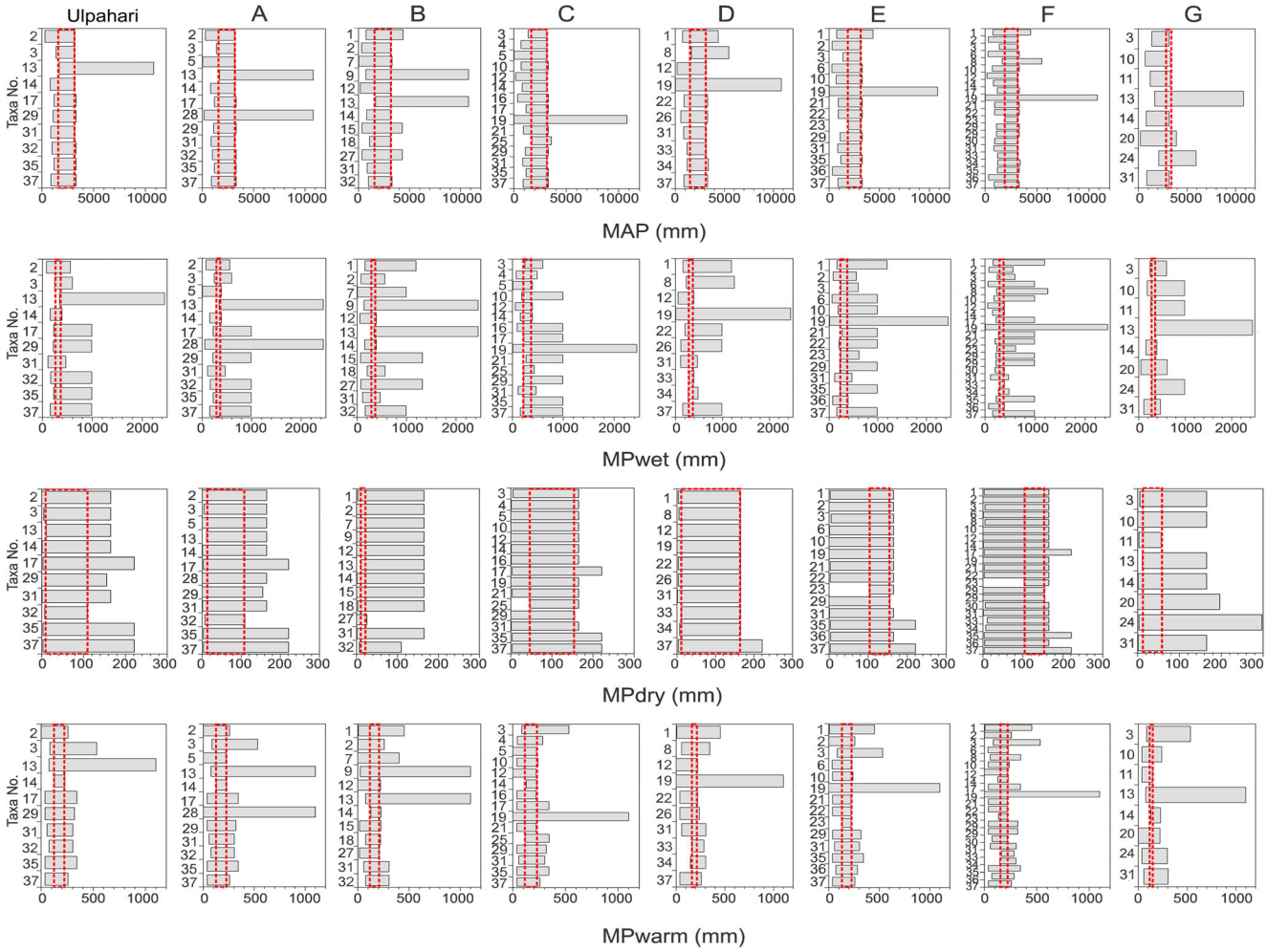

Fig. 4 The coexistence intervals of precipitation parameters (MAP, MPwet, MPdry, and MPwarm) of the fossil wood assemblages (vertical red lines indicate common range for all the NLRs)

Eastern margin of the BB

Khowai District assemblage (D)

Wood assemblages of Khowai and Teliamura (late Miocene −Pliocene) from Tripura are grouped under the Khowai District assemblage (Table 3), which exhibits 14 species under eight families. Fabaceae (36%) members are found abundantly in the assemblage, along with some others such as Sonneratiaceae, Celastraceae, Lythraceae, Sapotaceae, and Sapindaceae. The most dominant elements are tropical moist to dry deciduous forest taxa (31%). Members of tropical moist evergreen forests (15%) are represented by *Palaquium* (Sapotaceae), *Bouea* spp. (Anacardiaceae), and *Isoberlinia* (Fabaceae). On the other hand, tropical moist deciduous types (15%) are represented by *Duabanga grandiflora* (Sonneratiaceae) and *Lagerstromia speciosa* (Lythraceae). Tidal coastal swampy (8%), tropical dry deciduous (8%) and semi-evergreen forest elements are also present (Fig. 2).

The CIs for this wood assemblage for MAT, MAP, WMT, CMT, MPwet, MPdry and MPwarm range between 26.1–27.7 °C, 1650–3151 mm, 27.5–28.1 °C, 22.2–27 °C, 300–389 mm, 11–165 mm, and 163–221 mm respectively (Table 3; Figs. 3 and 4).

West Tripura District assemblage (E)

Agartala, Baramura, Kunjaban, and Yogendranagar assemblages (late Miocene−Pliocene), when combined, comprise the West Tripura District assemblage. This combined assemblage consists of 21 xylotaxa (Tables 2, 3 and S1) from the families Anacardiaceae (*Gluta* and *Mangifera*), Fabaceae (*Albizia* spp., *Bauhinia*, *Millettia* and *Afzelia* or *Intsia*), Calophyllaceae (*Calophyllum*), Combretaceae (*Terminalia*), Dipterocapaceae (*Anisoptera* and *Shorea robusta*), Sapindaceae (*Euphoria*), Sonneratiaceae (*Sonneratia*), and Thymelaeaceae (*Gonystylus*). In this wood assemblage the dominance of tropical moist to dry deciduous forest taxa

(45%) is evident. Other elements are tropical moist evergreen (25%), tidal coastal swampy (10%), tropical-subtropical evergreen (10%), tropical moist deciduous (5%), and semi-evergreen (5%) types (Tables 2, 3 and S1; Fig. 2).

Here, CIs suggest 26.5–27.6 °C for the MAT, 27.7–28.1 °C for the WMT, 25–27 °C for the CMT, 1930–3141 mm for the MAP, 270–389 mm for the MPwet, 103–155 mm for the MPdry, and 135–221 mm for the MPwarm (Table 3; Figs. 3 and 4).

Tripura assemblage (F)

This assemblage combines all the fossil wood taxa recovered from Udaipur, Melaghar, Manu Bazar, Bishalgarh, Laljuri, Amarpur, West Tripura, and Khowai districts of Tripura (Tables 2, 3 and S1; Fig. 2), and a late Miocene−Pliocene age is assigned for it. The dominant floral elements are Anacardiaceae (*Bouea*, *Gluta* and *Mangifera indica*), Celastraceae (*Lophopetalum littorale*), Combretaceae (*Terminalia*), Dipterocarpaceae (*Dipterocarpus* and *Shorea*), Fabaceae (*Bauhinia foveolata*, *Cynometra ramiflora*, *Isoberlinia* and *Millettia*), Lythraceae (*Lagerstroemia speciosa*), Sapindaceae (*Dimocarpus logan* and *Pometia*), Sapotaceae (*Palaquium*), Sonneratiaceae (*Duabanga grandiflora* and *Sonneratia apetala*), and Thymelaeaceae (*Gonystylus*). *Kayea assamica* (Clusiaceae), a submontane species, is also recorded in this assemblage (Table S1). Overall, the floristic analysis of the wood assemblage of the entire Tripura suggests a dominance of tropical moist to dry deciduous elements (41%) followed by tropical moist evergreen (17%) and tidal coastal swampy elements (14%). Other recovered types are tropical-subtropical evergreen (10%), tropical moist deciduous (6%), tropical moist deciduous to evergreen (4%), semi-evergreen (4%), and tropical dry deciduous (2%) elements.

In the entire wood assemblage of Tripura, CIs of the reconstructed climatic parameters range between 26.5–27.6 °C for MAT, 27.7–28.1 °C for WMT, 25–27 °C for CMT, 1930–3141 mm for MAP, 300–389 mm for MPwet, 103–155 mm for MPdry, and 135–221 mm for MPwarm (Table 3; Figs. 3 and 4).

Lalmai Hill assemblage (G)

The wood taxa recorded from Lalmai Hill Range, Comilla District, Bangladesh, belong to the Dupi Tila Formation (late Pliocene−early Pleistocene) and reveal a dominance of different members of Fabaceae (45%) such as *Cynometra*, *Copaifera*, *Detarium*, *Sindora*, *Kingiodendron*, and *Millettia prainii*. Other silicified wood taxa recovered are *Anisoptera* (Dipterocarpaceae), *Careya* (Lecythidaceae), *Chisocheton* (Meliaceae), *Calophyllum* (Clusiaceae), and *Artocarpus* (Moraceae). This wood assemblage shows a dominance of tropical moist to dry deciduous elements (34%), followed by tropical moist evergreen (33%), tropical moist deciduous to evergreen (22%), and tidal coastal swampy (11%) elements (Tables 2, 3 and S1; Fig. 2).

The CIs for this wood assemblage for MAT, MAP, WMT, CMT, MPwet, MPdry, and MPwarm range between 26.5–27.5 °C, 2099–3141 mm, 28.3–28.9 °C, 25–25.6 °C, 343–389 mm, 11–56 mm, and 128–146 mm respectively (Table 3; Figs. 3 and 4).

Discussion

Vegetation of the Bengal Basin during the late Miocene to early Pleistocene: spatial and temporal dynamics

Wood fossils are a reliable biotic proxy used in palaeovegetation and palaeoclimatic reconstructions, as information stored in petrified secondary woods almost remains unchanged through time and affords identification to their NLRs. Ecological preference of the NLRs facilitates understanding of their depositional settings (Prakash et al. 1994; Estrada-Ruiz et al. 2007; Jeong et al. 2009; Feng et al. 2010; Bamford 2011; Mehrotra et al. 2011; Tiwari et al. 2012). NLR analyses of the wood assemblages considered here show that during the late Miocene to early Pliocene, the most abundant components in the BB forests were: *Albizia*, *Afzelia/Intsia*, *Anisoptera*, *Artocarpus*, *Bauhinia*, *Bouea*, *Buchanania*, *Calophyllum*, *Careya*, *Cassia*, *Chisocheton*, *Cynometra*, *Dipterocarpus*, *Diospyros*, *Duabanga*, *Gluta*, *Isoberlinia*, *Kayea*, *Mangifera*, *Melanorrhoea*, *Millettia*, *Ormosia*, *Shorea*, *Sindora*, and *Terminalia*. Some less frequent taxa were: *Araucaria*, *Canarium*, *Dialium*, *Dracontomelum*, *Euphoria*, *Gonystylus*, *Kingiodendron*, *Koompassia*, *Lagerstroemia*, *Lannea*, *Phoebe*, *Lophopetalum*, *Mallotus*, *Pometia*, *Palaquium*, and members of Arecaceae. The dominant families were Fabaceae, Dipterocarpaceae, Anacardiaceae, Combretaceae, Clusiaceae, Sapindaceae, Celastraceae Burseraceae, Lythraceae, Sapotaceae, Sonnertiaceae, Lecythidaceae, Thymeliaceae, and Arecaceae. Most of these taxa are now constituents of the modern tropical forests of India and Bangladesh (Champion and Seth 1968). However, some warm temperate/sub-tropical and submontane taxa such as *Araucaria* sp. and *Kayea* spp. were also present in the assemblages.

Late Miocene to early Pliocene

The dominance of moisture-loving taxa over dry deciduous elements suggests that mainly a tropical moist deciduous forest occupied the entire BB during the late Miocene to early Pliocene. However, differences in abundances of drought-tolerant taxa express spatial variations. We see that such taxa

were more widespread at the western margin of the BB compared to its eastern part, while moisture-loving evergreen/semi-evergreen elements were more prevalent in the eastern part, indicating a moisture gradient from West to East, similar to, although weaker than, the modern one that is influenced by a strong ISM in the eastern part of the region. At present, tropical dry deciduous forest prevails in the western part of the basin, compared with moist deciduous/semi-evergreen forests in its eastern part. Thus, it may be inferred that vegetation of the western part of the basin has undergone more pronounced changes since the early Pliocene, compared to its eastern part.

Late Pliocene to early Pleistocene

Of the seven wood assemblages, only the Lalmai Hill assemblage from the eastern part gives us insight into the late Pliocene to early Pleistocene vegetation of the BB. It is evident that Dipterocarpaceae, Moraceae, Meliaceae, Lecythidaceae, Calophyllaceae, and Fabaceae were dominant families of the BB forest during this time as well. Moisture-loving elements dominate the assemblage. This implies that a moist deciduous forest prevailed in this part of the basin during the late Pliocene to early Pleistocene as in present-day. Because there is no wood assemblage representing the late Pliocene to early Pleistocene vegetation of the western margin of the BB, it cannot be inferred when exactly moist-deciduous forests started transforming towards dry-deciduous ones at the western margin of the basin. In general, the late Pliocene is considered to mark the beginning of arid conditions that completely eradicated the Dipterocarpaceae from northern India and restricted this group to the northeastern and southwestern parts of the subcontinent (Sahni and Mitra 1980). This onset of aridification was accompanied by increasing continentality, due to the rise of the Himalaya and concomitant glaciations which perhaps led to a southward shift in the tropical forests (Mittre 1964; Sahni and Mitra 1980; Agarwal et al. 1989; Bhargava 2015). However, the presence of dipterocarps in late Pliocene to early Pleistocene Lalmai Hill assemblage indicates that Dipterocarpaceae were present in eastern India and thus points to a delay of aridification in this region.

Montane/submontane taxa are also documented in the late Miocene to early Pliocene BB wood assemblages. Elevation estimates of the Himalaya based on different methods indicate that the Himalaya achieved at least 5000 m elevation at 15 Ma, and then continued to rise to attain its present elevation (Garzione et al. 2000; Rowley et al. 2001; Saylor et al. 2009; Gébelin et al. 2013; Wang et al. 2014b; Ding et al. 2017; Spicer 2017). Thus, such montane/submontane taxa possibly were growing in the warm-temperate foothills of the Himalayan Mountains at the northern margin of the basin and might have been transported by rivers suggesting a strong rainfall regime.

The substantial presence of littoral and swampy elements in all of the late Miocene to early Pliocene wood assemblages considered here implies that the coast was not far away from the study areas. Probably, a landward shifting of the coastline took place during this time, all along eastern India as suggested by some earlier records from far eastern Indian sites (Lakhanpal 1970; Tiwari et al. 2012). Earlier geological and vertebrate fossil records suggest that there was a basin-ward decrease in sand content in various sedimentary formations of the BB during this time, and the entire basin became more marine in a general south-easterly direction (Mathur and Kohli 1964; Sahni and Mitra 1980). In the late Pliocene to early Pleistocene Lalmai Hill assemblage, tidal/coastal swampy elements occur in considerably lower diversity. This may indicate a southward shift of the coastline and retreat of tidal/coastal swampy plant communities during this phase.

Climate of the Bengal Basin during the late Miocene to early Pleistocene: spatial and temporal trends

The anatomical characters of the fossil woods provide an insight into the climatic conditions of the BB during the late Miocene to early Pleistocene. All recovered silicified woods of the BB are diffused porous woods with indistinct growth rings and medium to large sized vessels with uniform diameters. Woods with indistinct growth rings indicate a tropical climate with low temperature seasonality (Wheeler and Baas 1993), so such an environmental condition must have existed in the BB during the time of deposition. In addition, large but infrequent vessels are also indicators of tropical climate (Wheeler and Baas 1993). The occurrence of scalariform perforations on vessel walls is found to be relatively high in cool temperate to arctic and tropical high montane climatic conditions, but rare in tropical lowland floras (Wheeler and Baas 1993), and simple perforation plates facilitate efficient water transport (Wheeler and Baas 1993). Hence, the dominance of simple perforation plate in BB woods also indicates a high rainfall regime. Moreover, the high incidence of paratracheal parenchyma with homocellular and storied arrangement of ray cells in the wood tissues also suggest a high temperature environment (Wolfe and Upchurch 1987; Woodcock and Ignas 1994; Tiwari et al. 2012). Thus, presence of the above characters in some taxa of the BB wood assemblages is again indicative of a warm tropical climatic condition (Woodcock and Ignas 1994) (Table S5). Moreover, the high 'V' values (> 1) for all the BB fossil woods, including the swampy and littoral elements, imply that these plants were under low water stress condition during the time of deposition (Carlquist 1988) (Table S5). Likewise, a higher value of mesomorphy also suggests that the plants were adapted to humid conditions, with high soil-available water (due to rainfall) (Carlquist 1977) (Table S5). Though, during the late Miocene to early Pliocene, the coast was nearby the study areas in the BB, yet

coastal and swampy taxa did not suffer much due to exposures to saline ground water conditions as reflected by their high 'V' and 'M' values. The low water stress for the coastal/swampy taxa may be attributable to high rainfall-induced surface run-off, ground water flow, and river inputs which perhaps flushed out salt from the tidal flat (Schmitz et al. 2006 and references therein), thus explaining the low water stress as reflected by 'V and 'M' indices. Overall, a warm tropical climate with low seasonality of temperature and high precipitation prevailed in the BB during the time of deposition.

However, no spatial and temporal trends are revealed in our qualitative data. Based on CA quantifications a minor temperature gradient from the western to eastern margin of the BB existed during the late Miocene to early Pliocene as can be inferred by comparing the CIs of the reconstructed climatic parameters (Table 3). Western sites show slightly lower CI boundaries for MAT than those of the eastern part of the basin, with a difference of about 1–2 °C while the upper bounds show a similar trend (Table 3). When compared with modern MAT, western sites show a close to present-day MAT, but the sites at the eastern margin show a considerably higher-than-present mean annual temperature. For summer temperatures, both the western and eastern sites show similar and near to modern values, while winter temperatures were higher than today and even warmer at the eastern side of the basin. During the late Miocene to early Pliocene, temperatures across the BB were more equable and the seasonality of temperature was lower in the entire basin compared with the present. Nevertheless, temperature seasonality was more pronounced in the West compared to the East.

For the late Pliocene to early Pleistocene, only one site in the eastern part of the BB is available and results from that show a higher-than-modern MAT (Tables 3, S5 and S6). Comparing MART values, here a more marked temperature seasonality than earlier becomes evident, though it was still weaker than today. A post-late Pliocene–early Pleistocene cooling in MAT of c. 1–1.5 °C (Tables 3, S5 and S6) may correspond to the global cooling trend following the onset of Northern Hemispheric Glaciations after the late Pliocene (Shackleton et al. 1988; Maslin et al. 1998; Zachos et al. 2001). Our results imply that, in general, the BB climate followed the global temperature trend since the late Miocene, but the observed minor spatial differences may be attributable to regional variability.

Precipitation estimates suggest that during the late Miocene to early Pliocene, MAP was notably higher across the entire BB than at present. However, a spatial pattern can also be recognised, with eastern sites experiencing higher annual rainfall than the western part of the BB. A significant difference between MPwet and MPdry values, and a corresponding high MARP in all the sites studied, indicate a distinct seasonality of precipitation, characteristic of a monsoonal climate. A higher MARP during the late Pliocene–early Pleistocene than earlier also implies an intensification of the monsoonal regime. However, MSI values suggest that in contrast to the present, monsoon intensity was comparably weak in the BB across the late Miocene to early Pleistocene (Tables S5 and S6), which may be a function of a wetter-than-present dry season.

An insight into the Asian monsoonal climate during the late Miocene to early Pleistocene

The modern Asian monsoon (AM) system has two components, i.e. the East Asian monsoon or East Asian Summer Monsoon (EASM) and the South Asian monsoon (SAM) or Indian summer monsoon (ISM) (Molnar et al. 2010). These two components together control precipitation over mainland Asia. The variability of these two components of the AM has been widely investigated and evoked many debates (Sun and Wang 2005; Wan et al. 2007; Clift et al. 2008; Tang et al. 2011; Yao et al. 2011). Two other significant agents of the Asian climate system are mid-latitude Subtropical Westerly Jet (SWJ) or western disturbances (WD) and the East Asian winter monsoon (EAWM). WDs bring extreme precipitation during the winter season over Central Asia including the northern and central parts of the Himalaya and northern India, due to orographic land-atmosphere interactions (Dimri et al. 2015). The EAWM refers to an extremely cold and dry atmospheric flow over Asia corresponding to the eastward and southward movement of cold air from the Siberian High (Luo and Zhang 2015). To achieve an understanding of the late Miocene to early Pleistocene monsoonal climate of Asia we compare BB data with some quantitative climate data from sites chiefly influenced by either ISM or EASM/EAWM (Figs. 5, 6, and 7; Tables S5 and S6). This will provide insight into the late Miocene to early Pleistocene climate variability in Asia and its causal mechanism(s).

For the late Miocene-early Pliocene, most of the ISM and EASM sites show warmer-than-present mean annual temperatures (Figs. 5, 6, and 7; Tables S5, S6) corroborating the global post-MMCO (Mid-Miocene Climatic Optimum) warm conditions that continued until the late Miocene, except at some sites situated in southeast China. The lower MATs in southeast China were primarily a function of cooler winter temperatures (Tables S5, S6) and may be attributed to a late Miocene strengthening of the EAWM. Planktic and benthic $\delta^{18}O$ signals of ODP core 1146 (Ocean Drilling Program) from the South China Sea also point towards a sustained cooling trend that began between 7.1 and 6.9 Ma and continued until c. 5.7 Ma (Holbourn et al. 2018). This cooling may be due to a southward shift of the average summer position of the Intertropical Convergence Zone (ITCZ) that minimised the influence of tropical convection and intensified dry winter monsoon over Southeast Asia (Holbourn et al. 2018). Though an earlier record (Ohneiser et al. 2015) linked this cooling episode to the increase of Antarctic ice volume, the Site

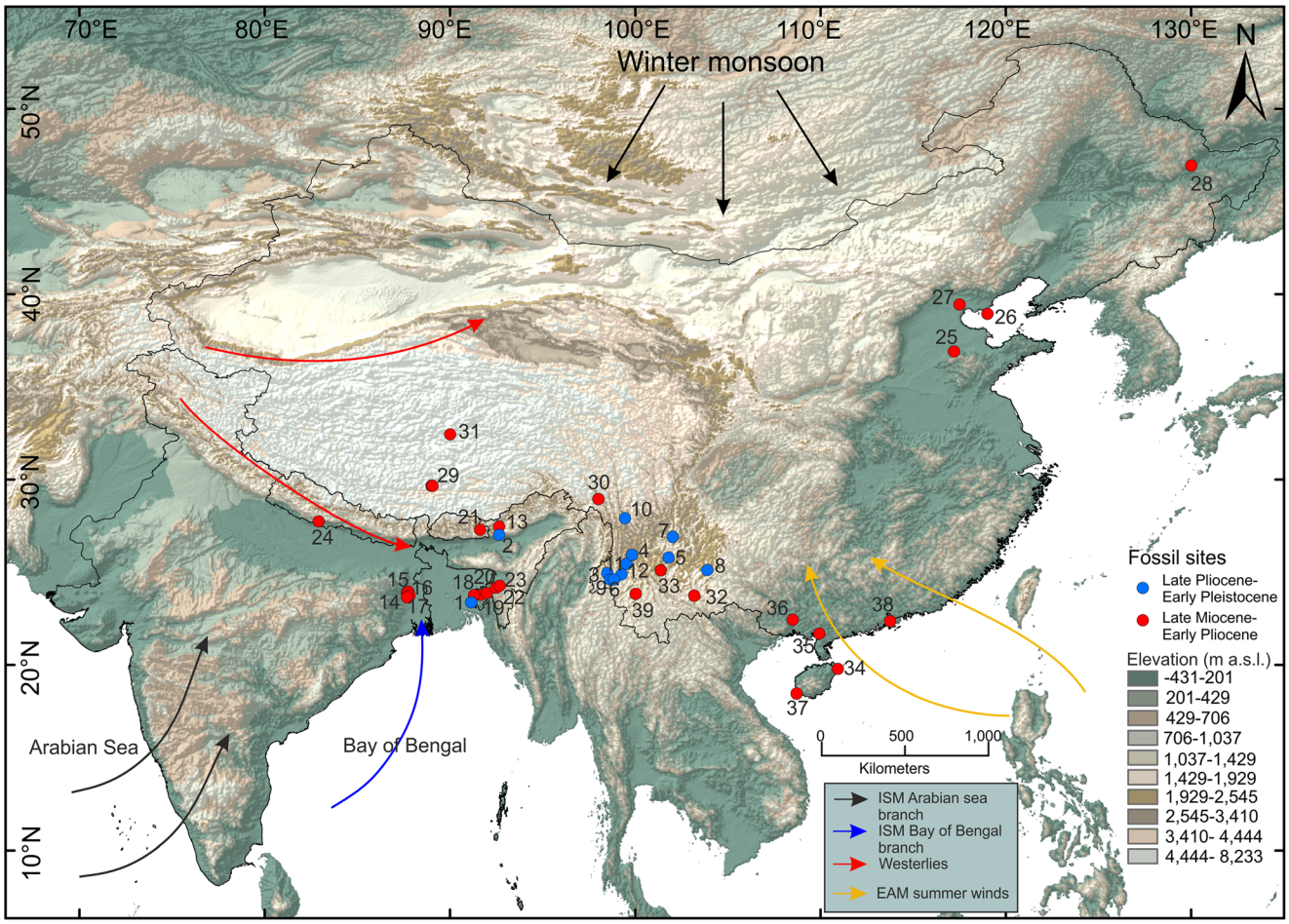

Fig. 5 Elevation map of southern Asia showing the positions of key fossil localities discussed in this study and the directions of major wind patterns associated with South Asia, i.e. Indian summer monsoon (ISM) and East Asian Monsoon (EAM) in summer, winter monsoon and Westerlies. For details on the fossil sites, please see Supplementary Tables S5 and S6

1146 data connect it to a massive Northern Hemisphere cooling down to subtropical latitudes (Holbourn et al. 2018). However, some northeast Chinese sites do not show any significant changes in MAT since the late Miocene, and also no such impact of a strong southeast winter monsoon is evident. This incongruity may be due to the low diversity of fossil pollen assemblages in some of these sites, which may fail to capture temperature fluctuations, or may be due to poor age assignments for some of those assemblages (Liu et al. 2011).

Sites situated either on the present-day Tibetan Plateau (TP) or its southeastern boundary also need special attention. Modern-day MATs of these sites are very low compared with those in the late Miocene (Tables S5, S6). In general, surface temperature gradients are correlated to latitude and altitude. Best examples of latitudinal temperature differences are visible in the Mio-Pliocene temperature trends of southern ISM/EASM sites and northern EASM sites (Figs. 5, 6, and 7; Tables S5 and S6). However, for the TP and its surroundings, probably altitudinal differences drove significant changes in temperatures during the late Miocene to early Pleistocene, as significant growth in the TP region took place across the Neogene, due to rise of the valley floor through a combination of compressional uplift and sediment fill which helped TP attaining the height of the bounding mountains (Molnar 2005; Yao et al. 2011; Spicer 2017; Spicer et al. 2020).

The late Pliocene–early Pleistocene time was also warm in Asia although with spatial variability, where south Asian sites were warmer than the Southeast Asian sites. A rapid southeasterly growth of the Qinghai–TP may explain this incongruity (Molnar 2005; Yao et al. 2011; Huang et al. 2015; Spicer 2017; Spicer et al. 2020). Based on the MART values, a more distinct seasonality of temperature can be inferred for the Plio-Pleistocene than for the Mio-Pliocene in both, southern and eastern Asia (Figs. 5, 6, and 7; Tables S5 and S6) which provides further evidence for a general cooling trend, which may be attributable to the rapid growth of the TP region in some places and a post late Pliocene global cooling trend following the onset of Northern Hemispheric Glaciations,

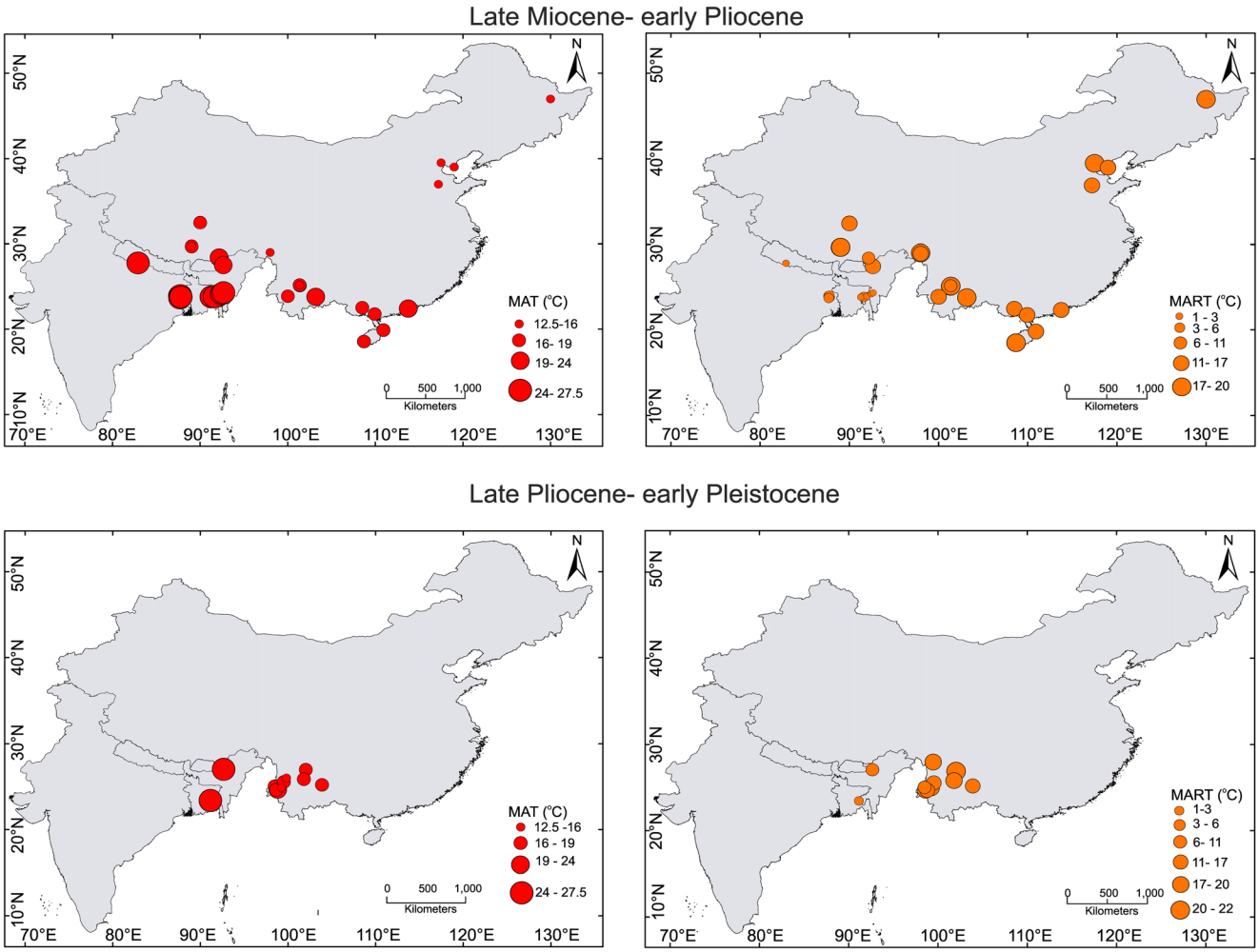

Fig. 6 MAT and MART variations in southern Asia during the late Miocene to early Pleistocene

among others (Shackleton et al. 1988; Maslin et al. 1998; Zachos et al. 2001; Spicer et al. 2020).

With respect to precipitation, a comparison of MAP values reveals overall very humid conditions both in the ISM or EASM sites suggesting strong late Miocene Indian and East Asian monsoons (Zheng et al. 2004). There are several theories for south Asian monsoon evolution, some records suggest that the Asian monsoon system predates the Miocene and even the onset of the India-Asia collision (Wang et al. 2014b; Renner 2016; Spicer 2017; Ingalls et al. 2018). Some climate modelling studies also inferred that monsoon would have existed in the whole of southern and southeastern Asia, even in the absence of a significant topography over Tibet, perhaps existed during the whole of the Cenozoic, or maybe even earlier, and might have generated due to seasonal migrations of the ITCZ (Huber and Goldner 2012; Spicer 2017). However, some recent studies suggest that orographic mechanical forcing, steering, and lifting were the dominant mechanisms for maintaining a strong precipitation over the Asia north of 30° N, and most likely the orographic changes in the Himalaya and TP regions would have acted as the modulators for the regional circulation and precipitation distribution (Curio and Scherer 2016; Reeves and Lin 2006; Wheeler et al. 2016; Acosta and Huber 2020). Further, the gradual changes in orography and extent of the Himalaya-TP region transformed an ITCZ-dominated monsoon to a sea-breeze dominated one during the late Neogene by acting as a mechanical barrier to dry-cold continental air advecting into the south and southeast Asian landmass which also enhanced the influence of moist air from the Indian Ocean/South China Sea (Farnsworth et al. 2019). The projection of the high (> 5 km) Himalaya above the Tibetan highlands at around 15 Ma coincides with the onset of a circulation system that became modern ISM (Spicer 2017). So probably the ISM in its modern form developed after the mid-Miocene when the rising Himalaya increasingly created an obstacle to north-south airflows (Spicer 2017). Also, the evolution of the EASM has been linked to the rise of large parts of northern Tibet (Liu and Dong 2013). Other causal factors for EASM intensification may be a strong winter Siberian high pressure zone as global temperatures declined, or an intensification of the cross-equatorial pressure gradient between an atmospheric

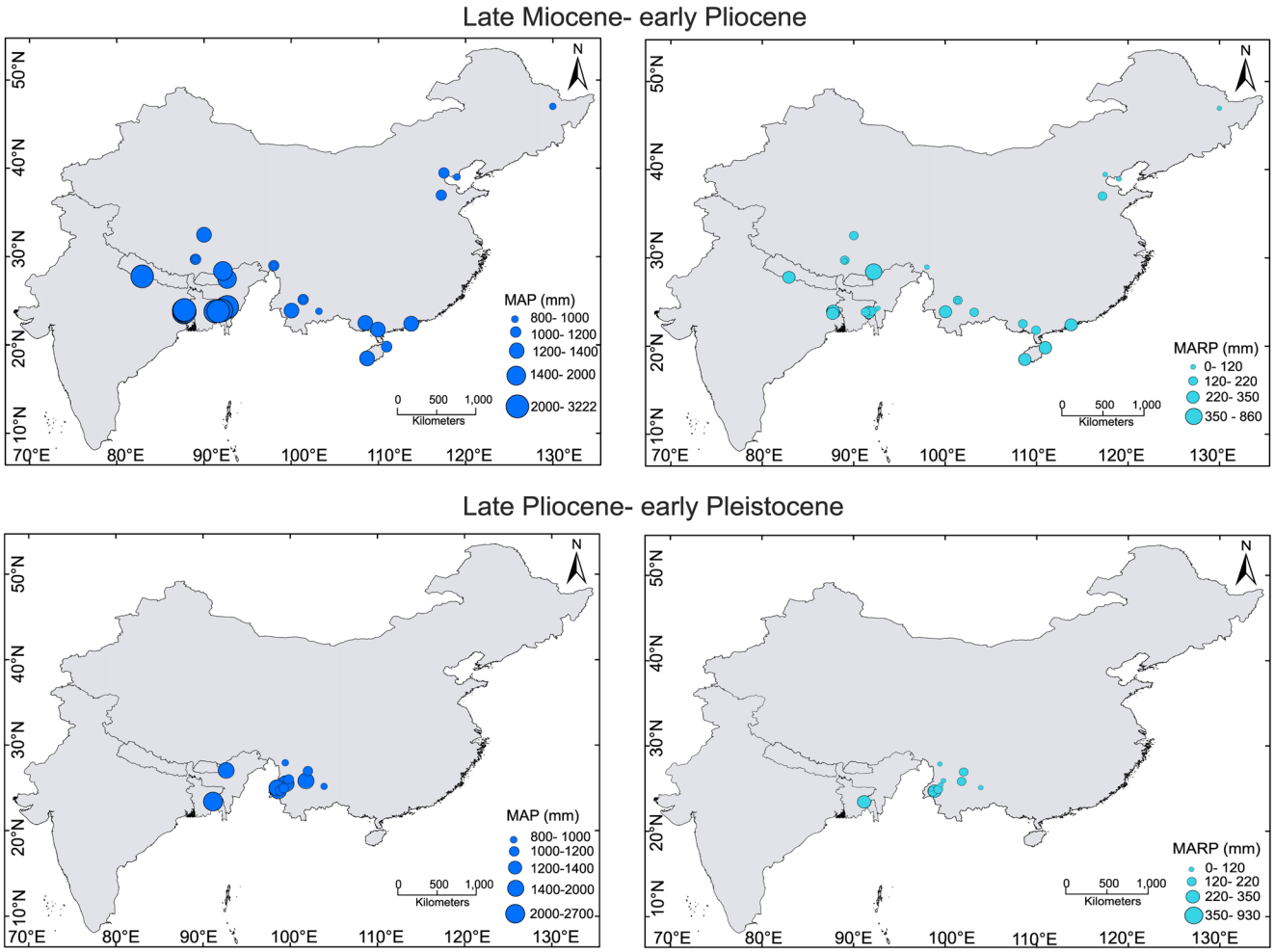

Fig. 7 MAP and MARP variations in Southern Asia during the late Miocene to early Pleistocene

high-pressure cell over Australia and a low-pressure cell over mid-latitude East Asia, or intensification of the cross-equatorial sea-surface temperature (SST) gradient due to progressive Antarctic glaciations (Ao et al. 2016; Spicer 2017). A recent climate modelling study indicates that the weakening of the Walker circulation, associated shoaling of the eastern Pacific thermocline, and strengthening of easterlies also coincide well with the enhancement in EASM precipitation during the Neogene (Farnsworth et al. 2019).

In contrast to the present-day, monsoon intensity was weaker in the late Miocene–early Pliocene in both the ISM and EASM sites, though MAP was higher suggesting a year-round high humidity, possibly due to a more humid dry season (Tables S5 and S6; Hazra et al. 2020). An overall decrease in precipitation after the Pleistocene has been noticed in both the ISM and EASM sites which may be an early Pleistocene phenomenon of global monsoonal decline (Tables S5 and S6). The MARP values show a higher seasonality in the southern Asian sites and a lower seasonality in the northern sites (Tables S5 and S6; Fig. 7). For example, a wetter-than-modern late Pliocene western Yunnan has been linked to the continuous uplift of mountains in western Yunnan, as well as the intensification of the EAWM, both occurring concurrently in the post-Pliocene period (Su et al. 2013).

Palaeoclimate estimates derived from the BB wood flora for the late Miocene to early Pleistocene time-span and their comparison with some southern and southeast Asian ISM and EASM records help to understand the climate trends and the interrelationships between the ISM, EASM and EAWM, the dominant components of the AM. Our results suggest that the BB climate followed a global temperature trend where, in congruity with most of the south and southeast Asian records, a warmer-than-present Mio-Pliocene is apparent. The following post-late Pliocene cooling may be attributed to the Northern Hemispheric Glaciations. Similarly, a comparison of BB precipitation estimates with other records points towards an apparent monsoonal regime during the Mio-Pliocene in both the ISM and EASM sites, however, monsoon intensity was weaker than now. Several theories are there which may link this monsoon to Miocene orogenic changes of the Himalaya-TP that may have affected ISM intensity, or seasonal migrations of the ITCZ. For EASM it may be a

strong winter Siberian high pressure zone, due to decline in global temperatures or an intensification of the cross-equatorial pressure gradient between an atmospheric high-pressure cell over Australia and a low-pressure cell over mid-latitude East Asia, or intensification of the cross-equatorial sea-surface temperature (SST) gradient due to progressive Antarctic glaciations or a weakening of the Walker circulation and a shoaling of the eastern Pacific thermocline with strengthening of easterlies. However, to validate these theories and to build a clearer understanding on the AM evolution we need more high resolution proxy climate data from both south and southeast Asia.

Conclusions

Fossil wood data provide a detail insight into the spatial and temporal variations in vegetation and climate of the BB during the late Miocene to early Pleistocene. It is observed that the late Miocene–early Pliocene forests were dominated by moist deciduous/semi-evergreen/evergreen elements. During the late Pliocene–early Pleistocene moisture-loving elements decreased considerably. The vegetation of the western margin of the basin has altered more profoundly than its eastern part. BB wood data reveal that during the late Miocene–early Pliocene, the western margin of the basin was slightly cooler than today, both in terms of mean annual temperature (MAT) and summer temperature, though winters were warmer than now. At the same time, sites at the eastern margin show a summer temperature similar to present-day, a higher MAT and a warmer winter temperature. Mean annual precipitation (MAP) was higher compared with the present at both margins of the basin. Later, during late Pliocene–early Pleistocene, climates were also warmer than now with respect to MAT, summer and winter temperatures. MAP during this time was also higher than now. However, the decline of MAP towards present-day is more pronounced in the western than the eastern part of the basin. Monsoon intensity was weaker during the time period from late Miocene to early Pleistocene than it is now.

The comparison of our results with modern climate data and earlier records of ISM and EASM provides insights into the south/southeast Asian climate during the late Neogene–Quaternary transition. In general, a drop in temperature and a weakening in ISM strength since the early Pleistocene corroborate the global cooling trend, though with spatial differences. All EASM sites also show similar trends as in the ISM sites, except for the southeastern part of China.

Acknowledgements RG acknowledges the Director, Birbal Sahni Institute of Palaeosciences, Lucknow, for her encouragement, support and permission to publish this work. SB, AB, IS and DKP acknowledge UGC-CAS, Phase VII, Department of Botany, University of Calcutta, for the infrastructural facilities. This work is a contribution to NECLIME (Neogene Climate Evolution in Eurasia) and the ROCEEH (The Role of Culture in Early Expansions of Humans) Research Centre of the Heidelberg Academy of Sciences and Humanities. We thank Professor Robert A. Spicer, The Open University, UK and an anonymous reviewer for their constructive suggestions on this manuscript which certainly have increased the merit of this work.

Compliance with ethical standards

Conflict of interest The authors declare that they have no conflict of interest.

References

Acharya, S., & Roy, S. K. (1986). Fossil woods of Leguminosae from the Tertiary of Tripura, India. *Burdwan University Journal of Science, 3*(1), 127–132.

Acosta, R. P., & Huber, M. (2020). Competing topographic mechanisms for the summer Indo-Asian monsoon. *Geophysical Research Letters, 47*, e2019GL085112. https://doi.org/10.1029/2019GL085112.

Agarwal, D. P., Dodia, R., Kotlia, B. S., Razdan, H., & Sahni, A. (1989). The Plio-Pleistocene geologic and climatic record of the Kashmir volley, India: A review and new data. *Palaeogeography, Palaeoclimatology, Palaeoecology, 73*, 267–286.

Agarwal, A., Ambwani, K., Saha, S., & Kar, R. K. (2000). Fossil wood of *Barringtonia* (Lecythidaceae) from Ramgarh, Chittagong Hill Tract, Bangladesh. *Phytomorphology, 50*(3,4), 333–336.

Alam, M. (1989). Geology and depositional history of Cenozoic sediments of the Bengal Basin of Bangladesh. *Palaeogeography, Palaeoclimatology, Palaeoecology, 69*, 125–139.

An, Z. S., Kutzbach, J. E., Prell, W. L., & Porter, S. C. (2001). Evolution of Asian monsoons and phased uplift of the Himalaya—Tibetan Plateau since Late Miocene times. *Nature, 411*, 62–66.

Ao, H., Roberts, A. P., Dekkers, M. J., Liu, X., Rohling, E. J., Shi, Z., An, Z., & Zhao, X. (2016). Late Miocene–Pliocene Asian monsoon intensification linked to Antarctic ice-sheet growth. *Earth and Planetary Science Letters, 444*, 75–87.

Ash, S. R., & Creber, G. T. (1992). Palaeoclimatic interpretation of the wood structures of the trees in the Chinle Formation (Upper Triassic), Petrified Forest National Park, Arizona, USA. *Palaeogeography, Palaeoclimatology, Palaeoecology, 96*, 299–317.

Awasthi, N., Mehrotra, R. C., & Bhattachryya, A. (1994). Fossil wood of *Cynometra* from the Neogene of Tripura. *Geophytology, 23*, 291–293.

Baas, P., & Wheeler, E. A. (2011). Wood anatomy and climate change. Chapter 6. In *Climate change, ecology and systematics systematics association special volume series* (pp 141-155). Cambridge University Press. https://doi.org/10.1017/CBO9780511974540.007.

Bamford, M. K. (2011). Late Pliocene woody vegetation of area 41, Koobi flora, East Turkana Basin, Kenya. *Review of Palaeobotany and Palynology, 164*, 191–210.

Bande, M. B., & Prakash, U. (1980). Fossil woods from the Tertiary of West Bengal, India. *Geophytology, 10*, 146–157.

Bande, M. B., & Srivastava, G. P. (1989). Fossil woods of Guttiferae (*Kayea*) and Lauraceae from the Tertiary of West Bengal. *Geophytology, 18*(2), 217–218.

Banerji, R. K. (1984). Post-Eocene Biofacies, Palaeoenvironments and Palaeogeography of the Bengal Basin, India. *Palaeogeography, Palaeoclimatology, Palaeoecology, 45*, 49–73.

Bera, S., & Banerjee, M. (1990). A new species of *Palmoxylon* and accretionary structures in the petrified woods from lateritic sediment in the western part of Bengal basins, India. *Indian Journal of Earth Sciences, 17*, 78–89.

Bera, S., & Banerjee, M. (1997). *Palmoxylon pantii* Trivedi & Surange from Santiniketan, West Bengal. *Geobios New Reports, 16*, 60–62.

Bera, S., & Banerjee, M. (2001). Petrified wood remains from Neogene sediments of the Bengal Basin, India with remarks on palaeoecology. *Palaeontographica Abteilung B, 260*, 167–199.

Bera, S., Parua, D., & Sen, I. (2000). Fossil wood resembling *Sindora* Miq. from the Neogene of West Bengal, India. *Indian Journal of Earth Sciences, 1–4*, 26–31.

Bhargava, O. N. (2015). Evolution of the tethyan and karewa successions in Kashmir: A synthesis. *Journal of the Palaeontological Society of India, 60*(1), 51–72.

Biswas, A., Khan, M. A., & Bera, S. (2019). Occurrence of Dryobalanops Gaertn. (Dipterocarpaceae) in the late Miocene of Bengal basin, India and biogeography of the genus during the Cenozoic of Southeast Asia. *Botany Letters, 166*(4), 434–443. https://doi.org/10.1080/23818107.2019.1672102.

Carlquist, S. (1977). Ecological factors in wood evolution: A floristic approach. *American Journal of Botany, 64*, 887–896.

Carlquist, S. (1988). *Comparative wood anatomy: Systematic, ecological and evolutionary aspects of dicotyledon wood*. Berlin: Springer.

Cerling, T. E., Wang, Y., & Quade, J. (1993). Expansion of C_4 ecosystems as indicator of global ecological change in the late Miocene. *Nature, 361*, 344–345.

Cerling, T. E., Harris, J. M., MacFadden, B. J., Leakey, M. G., Quade, J., Eisenmann, V., & Ehleringer, J. R. (1997). Global vegetation change through the Miocene–Pliocene boundary. *Nature, 389*, 153–158.

Champion, H. G., & Seth, S. K. (1968). *A revised survey of the forest types of India* (pp. 404). Delhi: Manager of Publications.

Chatterjee, L. (1970). The climate of West Bengal-A genetic approach. In A. B. Chatterjee, A. Gupta, & P. K. Mukhopadhyay (Eds.) *West Bengal*. (pp. 42–47). Calcutta: Presidency College, Geographical Institute.

Chowdhury, K. A., & Tandon, K. N. (1952). A new record for the fossil wood of *Glutoxylon* from the southern part of West Bengal. *Current Science, 21*(6), 161.

Clift, P. D., Hodges, K. V., Heslop, D., Hannigan, R., Van Long, H., & Calves, G. (2008). Correlation of Himalayan exhumation rates and Asian monsoon intensity. *Nature Geoscience, 1*, 875–880.

Creber, G. T., & Chaloner, W. G. (1984). Influence of environmental factors in the wood structure of living and fossil trees. *Botanical Review, 50*, 357–448.

Curio, J., & Scherer, D. (2016). Seasonality and spatial variability of dynamic precipitation controls on the Tibetan Plateau. *Earth System Dynamics, 7*(3), 767–782. https://doi.org/10.5194/esd-7-767-2016.

Cutler, D. F., & Gregory, M. (1998). *Anatomy of Dicotyledons. Volume IV. Saxifragales* (p. 324). Oxford: Clarendon Press.

Dam, J. A. van (2006). Geographic and temporal patterns in the late Neogene (12–3 Ma) aridification of Europe: The use of small mammals as paleoprecipitation proxies. *Palaeogeography, Palaeoclimatology, Palaeoecology, 238*, 190–218.

Deb, U., & Ghosh, A. K. (1974). On the occurrence of *Terminaloxylon*, an angiospermous fossil wood from the victinity of Shantiniketan, Birbhum District, West Bengal. *Indian Journal of Earth Sciences, 1*(2), 208–213.

Dimri, A. P., Niyogi, D., Barros, A. P., Ridley, J., Mohanty, U. C., Yasunari, T., & Sikka, D. R. (2015). Western disturbances: A review. *Reviews of Geophysics, 53*, 225–246.

Ding, L., Spicer, R. A., Yang, J., Xu, Q., Cai, F., Li, S., Lai, Q., Wang, H., Spicer, T. E. V., Yue, Y., Shukla, A., Srivastava, G., Khan, M. A., Bera, S., & Mehrotra, R. (2017). Quantifying the rise of the Himalaya orogen and implications for the South Asian monsoon. *Geology, 45*, 215–218.

Estrada-Ruiz, E., Martinez-Cabrera, H. I., & Cevallos-Ferriz, S. R. S. (2007). Fossil woods from the late Campanian–early Maastrichtian Olmos Formation, Coahuila, Mexico. *Review of Palaeobotany and Palynology, 145*, 123–133.

Farnsworth, A., Lunt, D. J., Robinson, S. A., Valdes, P. J., Roberts, W. H. G., Clift, P. D., Markwick, P., Su, T., Wrobel, N., Bragg, F., Kelland, S.-J., & Pancost, R. D. (2019). Past East Asian monsoon evolution controlled by paleogeography, not CO_2. *Science Advances, 5*, eaax1697.

Feng, X. X., Yi, T. M., & Jin, J. H. (2010). First record of *Paraphyllanthoxylon* from China. *IAWA Journal, 31*, 89–94.

Francis, J. E. (1984). The seasonal environment of the Purbeck (UpperJurassic) fossil forests. *Palaeogeography, Palaeoclimatology, Palaeoecology, 48*, 285–307.

Gani, M. R., & Alam, M. M. (2003). Sedimentation and basin-fill history of the Neogene clastic succession exposed in the southeastern fold belt of the Bengal Basin, Bangladesh: A high-resolution sequence stratigraphic approach. *Sedimentary Geology, 155*, 227–270.

Garzione, C. N., Quade, J., DeCelles, P. G., & English, N. B. (2000). Predicting paleoelevation of Tibet and the Himalaya from $\delta^{18}O$ vs. altitude gradients of meteoric water across the Nepal Himalaya. *Earth and Planetary Science Letters, 183*, 215–219.

Gébelin, A., Mulch, A., Teyssier, C., Jessup, M. J., Law, R. D., & Brunel, M. (2013). The Miocene elevation of Mount Everest. *Geology, 41*, 799–802.

Ghosh, S. S., & Kazmi, M. H. (1961). *Pahudioxylon sahnii* sp. nov.—A fossil record from the Miocene (?) of Tripura. *Scientific Culture, 27*, 96–98.

Ghosh, P. K., & Roy, S. K. (1978). Fossil wood of *Canarium* from the Tertiary of West Bengal, India. *Current Science, 47*(21), 804–805.

Ghosh, P. K., & Roy, S. K. (1979a). A fossil wood of *Dracontomelum* from the Tertiary of West Bengal, India. *Current Science, 48*, 362.

Ghosh, P. K., & Roy, S. K. (1979b). *Dipterocarpoxylon bolpurense* sp. nov., a fossil wood of Dipterocarpaceae from the Miocene of Bolpur. Birbhum District.West Bengal. *Current Science, 48*(11), 495–496.

Ghosh, P. K., & Roy, S. K. (1979c). *Chistochetonoxylon bengalensis* gen. et sp. nov., a new fosil wood of Meliaceae from the Tertiary beds of Birbhum District, West Bengal, India. *Current Science, 48*(16), 737–739.

Ghosh, P. K., & Roy, S. K. (1979d). A new species of *Calophyllum* from the Miocene beds of Birbhum District, West Bengal, India. *Current Science, 48*(18), 823–824.

Ghosh, P. K., & Roy, S. K. (1980). Fossil wood of *Anisoptera* from the Miocene beds of Birbhum District, West Bengal, India. *Current Science, 49*(17), 665–666.

Ghosh, P. K., & Roy, S. K. (1981). *Cassinium ballavpurense* sp. nov. from the Miocene of West Bengal, India. *Acta Botanica Indica, 9*, 285–289.

Ghosh, P. K., & Roy, S. K. (1982). Fossil woods of Caesalpinoidae from the Miocene of West Bengal, India. *Acta Botanica Indica, 10*, 50–55.

Ghosh, S. S., & Taneja, K. K. (1961). Further record of *Glutoxylon* from the Miocene (?) of Tripura. *Scientific Culture, 27*, 581–582.

Han, W.-X., Fang, X.-M., & Berger, A. (2012). Tibet forcing of mid-Pleistocene synchronous enhancement of East Asian winter and summer monsoons revealed by Chinese loess record. *Quaternary Research, 78*, 174–184.

Hass, H., & Rowe, N. P. (1999). Thin section and wafering. In T. P. Jones & N. P. Rowe (Eds.), *Fossil plants and spores, modern techniques* (pp. 76–81). London: Geological Society.

Hazra, T., Spicer, R. A., Hazra, M., Mahato, S., Spicer, T. E. V., Bera, S., Valdes, P. J., Farnsworth, A., Hughes, A. C., Jiang, Y., & Khan, M. A. (2020). Latest Neogene monsoon of the Chotanagpur Plateau, eastern India, as revealed by fossil leaf architectural signatures. *Palaeogeography, Palaeoclimatology, Palaeoecology, 545*. https://doi.org/10.1016/j.palaeo.2020.109641.

Herzschuh, U., Birks, H. J. B., Mischke, S., Zhang, C., & Böhner, J. (2010). A modern pollen–climate calibration set based on lake sediments from the Tibetan Plateau and its application to a Late Quaternary pollen record from the Qilian Mountains. *Journal of Biogeography, 37*, 752–766.

Holbourn, A. E., Kuhnt, W., Clemens, S. C., Kochhann, K. G. D., Jöhnck, J., Lübbers, J., & Andersen, N. (2018). Late Miocene climate cooling and intensification of Southeast Asian winter monsoon. *Nature Communications, 9*, 1584. https://doi.org/10.1038/s41467-018-03950-1.

Huang, Y.-J., Chen, W.-Y., Jacques, F. M. B., Liu, Y.-S. C., Utescher, T., Su, T., Ferguson, D. K., & Zhou, Z.-K. (2015). Late Pliocene temperatures and their spatial variation at the southeastern border of the Qinghai–Tibet Plateau. *Journal of Asian Earth Sciences, 111*, 44–53.

Huber, B. T., & Goldner, A. (2012). Eocene monsoons. *Journal of Asian Earth Science, 44*, 3–23.

Hunday, A. (1954). On the newly found Tertiary patches in Bankura, West Bengal. *Scientific Culture, 19*, 245–246.

Hunday, A., & Banerjee, S. (1967). Geology and mineral resources of West Bengal. *Memoir Geological Survey of India, 97*, 1–302.

Ingalls, M., Rowley, D., Olack, G., Currie, B., Li, S., Schmidt, J., Tremblay, M., Polissar, P., Shuster, D. L., Lin, D., & Colman, A. (2018). Paleocene to Pliocene low-latitude, highelevation basins of southern Tibet: Implications for tectonic models of India-Asia collision, Cenozoic climate, and geochemical weathering. *GSA Bulletin, 130*, 307–330.

International Association of Wood Anatomists (IAWA). (1989). IAWA list of microscopic features for hardwood identification. *IAWA New Series, 10*, 219–332.

Jacques, F. M. B., Guo, S.-X., Su, T., Xing, Y.-W., Huang, Y.-J., Liu, Y.-S., Ferguson, D. K., & Zhou, Z.-K. (2011). Quantitative reconstruction of the late Miocene monsoon climates of southwest China: A case study of the Lincang flora from Yunnan Province. *Palaeogeography, Palaeoclimatology, Palaeoecology, 304*, 318–327.

Jacques, F. M. B., Shi, G., & Wang, W. M. (2013). Neogene zonal vegetation of China and the evolution of the winter monsoon. *Bulletin of Geosciences, 88*(1), 175–193.

Jansen, S., Baas, P., Gasson, P., Lens, F., & Smets, E. (2004). Variation in xylem structure from tropics to tundra: Evidence from vestured pits. *Proceedings of the National Academy of Science, 101*(23), 8833–8837.

Jeong, E. K., Kim, K., Suzuki, M., & Kim, J. W. (2009). Fossil woods from the lower coal bearing formation of the Janggi group (Early Miocene) in the Pohang Basin, Korea. *Review of Palaeobotany and Palynology, 153*, 124–138.

Khan, M. A., Spicer, R. A., Bera, S., Ghosh, R., Yang, J., Spicer, T. E. V., Guo, S.-X., Su, T., Jacques, F. M. B., & Grote, P. J. (2014). Miocene to Pleistocene floras and climate of the Eastern Himalayan Siwaliks, and new palaeoelevation estimates for the Namling–Oiyug Basin, *Tibet. Global and Planetary Change, 113*, 1–10.

Khan, M. A., Bera, M., Spicer, R. A., Spicer, T. E. V., & Bera, S. (2019). Palaeoclimatic estimates for a latest Miocene-Pliocene flora from the Siwalik Group of Bhutan: Evidence for the development of the South Asian Monsoon in the eastern Himalaya. *Palaeogeography, Palaeoclimatology, Palaeoecology, 514*, 326–335.

Kou, X.-Y., Ferguson, D. K., Xu, J.-X., Wang, Y.-F., & Li, C.-S. (2006). The reconstruction of palaeovegetation and palaeoclimate in the Late Pliocene of West Yunnan, China. *Climatic Change, 77*, 431–448.

Lacey, W. S. (1963). Palaeobotany technique. In J. D. Carthey & I. Duddington (Eds.), *Viewpoint in biology 2* (pp. 202–243). London: Butterworths.

Lakhanpal, R. N. (1970). Tertiary flora of India and their bearing on the historical geology of the region. *Taxon, 19*, 675–694.

Li, F. J., Rousseau, D. D., Wu, N. Q., Hao, Q. Z., & Pei, Y. P. (2008). Late Neogene evolution of the East Asian monsoon revealed by terrestrial mollusk record in Western Chinese Loess Plateau: From winter to summer dominated sub-regime. *Earth and Planetary Science Letters, 274*, 439–447.

Li, S.-F., Mao, L.-M., Spicer, R. A., Lebreton-Anberrée, J., Su, T., Sun, M., & Zhou, Z.-K. (2015). Late Miocene vegetation dynamics under monsoonal climate in southwestern China. *Palaeogeography, Palaeoclimatology, Palaeoecology, 425*, 14–40.

Lindsay, J. F., Holiday, D. W., & Hulbert, A. G. (1991). Sequence stratigraphy and the evolution of the Ganges–Brahmaputra complex. *American Association of Petroleum Geologists Bulletin, 75*, 1233–1254.

Liu, X. D., & Dong, B. W. (2013). Influence of the Tibetan Plateau uplift on the Asian monsoon arid environment evolution. *Chinese Science Bulletin, 58*, 4277–4291.

Liu, Y.-S. (. C.)., & Quan, C. (2016). Late Cenozoic climates of low-latitude East Asia: A paleobotanical example from the Baise basin of Guangxi, southern China. *Palaeoworld, 26*, 572–580.

Liu, X. D., & Yin, Z. Y. (2002). Sensitivity of east Asian monsoon climate to the uplift of the Tibetan Plateau. *Palaeogeography, Palaeoclimatology, Palaeoecology, 183*, 223–245.

Liu, Y.-S., Utescher, T., Zhou, Z.-K., & Sun, B. (2011). The evolution of Miocene climates in North China: Preliminary results of quantitative reconstructions from plant fossil records. *Palaeogeography, Palaeoclimatology, Palaeoecology, 304*, 308–317.

Lunt, D., Flecker, R., & Clift, P. D. (2010). The impacts of Tibetan uplift on palaeoclimate proxies. *Geological Society London Special Publications, 342*, 279–291.

Luo, X., & Zhang, Y. C. (2015). The linkage between upper-level jet streams over East Asia and East Asian Winter Monsoon variability. *Journal of Climate, 28*, 9013–9028.

Maslin, M. A., Li, X. S., Loutre, M. F., & Berger, A. (1998). The contribution of orbital forcing to the progressive intensification of Northern Hemisphere glaciation. *Quaternary Science Reviews, 17*(4–5), 411–426.

Mathur, L. P., & Kohli, G. (1964). Exploration and development for oil in India. Proc. 6th. *World Petroleum Congresses, 1*, 633–658.

Mehrotra, R. C., & Bhattacharyya, A. (2002). Wood of Dipterocarpus from a new locality of the Champanagar Formation of Tripura, India. *Palaeobotanist, 51*, 123–127.

Mehrotra, R. C., Bhattacharyya, A., & Shah, S. K. (2006). Petrified Neogene woods of Tripura. *Palaeobotanist, 55*, 67–76.

Mehrotra, R. C., Bera, S. K., Basumatary, S. K., & Srivastava, G. (2011). Study of fossil wood from the Middle–Late Miocene sediments of Dhemaji and Lakhimpur Districts of Assam, India and its palaeoecological and palaeophytogeographical implications. *Journal of Earth System Science, 120*, 681–701.

Mehrotra, R. C., Mehrotra, N., Srivastava, G., & Shah, S. K. (2017). Occurrence of fossil woods in the Unakoti District, Tripura and their palaeoclimatic significance. *Journal of the Palaeontological Society of India, 62*, 17–30.

Metcalfe, C. R., & Chalk, L. (1950). *Anatomy of Dicotyledons* (Vol. I and II). Oxford: Clarendon Press.

Metcalfe, C. R., & Chalk, L. (1987). *Anatomy of Dicotyledons Volume III, Magnoliales, Illiciales and Laurales* (2nd ed. pp. 1–240). Oxford: Oxford University Press.

Mittre, V. (1964). Floristic and ecological reconsiderations of the Pleistocene plant impressions from Kashmir. *Palaeobotanist, 13*(3), 308–327.

Molnar, P. (2005). Mio-Pliocene growth of the Tibetan Plateau and evolution of East Asian climate. *Palaeontologia Electronica, 8*(1), 2A.

Molnar, P., Boos, W. R., & Battisti, D. S. (2010). Orographic controls on climate and palaeoclimate of Asia: Thermal and mechanical roles for the Tibetan Plateau. *Annual Review of Earth and Planetary Science, 38*, 77–102.

Mosbrugger, V., & Utescher, T. (1997). The coexistence approach—A method for quantitative reconstructions of Tertiary terrestrial palaeoclimate data using plant fossils. *Palaeogeography, Palaeoclimatology, Palaeoecology, 134*, 61–86.

Mukherjee, A., Frayar, A. E., & Thomas, W. A. (2009). Geologic, geomorphic and hydrologic framework and evolution of the Bengal basin, India and Bangladesh. *Journal of Asian Earth Sciences, 34*, 227–244.

Ohneiser, C., Florindo, F., Stocchi, P., Roberts, A. P., DeConto, R. M., & Pollard, D. (2015). Antarctic glacio-eustatic contributions to late Miocene Mediterranean desiccation and reflooding. *Nature Communications, 6*, 8765.

Parrish, J. R., & Spicer, R. A. (1988). Middle Cretaceous wood from the Nanuskuk group, Central North Slope, Alaska. *Palaeontology, 31*, 19–34.

Poole, I., & Davies, C. (2001). *Glutoxylon* Chowdhury (Anacardiaceae) the first record of fossil wood from Bangladesh. *Review of Palaeobotany and Palynology, 113*, 261–272.

Prakash, U., Vaidyanathan, L., & Tripathi, P. P. (1994). Plant remains from the Tipam Sandstones of the North east India with remarks on the palaeoecology of the region during the Miocene. *Palaeontographica B, 231*, 113–146.

Qin, F., Ferguson, D. K., Zetter, R., Wang, Y. F., Syabryaj, S., Li, J., Yang, J., & Li, C.-S. (2011). Late Plicoene vegetation and climate of Zhangcun region, Shanxi, North China. *Global Change Biology, 17*, 1850–1870.

Quade, J., & Cerling, T. E. (1995). Expansion of C_4 grasses in the Late Miocene of Northern Pakistan: Evidence from stable isotopes in paleosols. *Palaeogeography Palaeoclimatology Palaeoecology, 115*, 91–116.

Reeves, H. D., & Lin, Y.-L. (2006). Effect of stable layer formation over the Po Valley on the development of convection during MAP IOP-8. *Journal of the Atmospheric Sciences, 63*(2003), 2567–2584. https://doi.org/10.1175/JAS3759.1.

Reimann, K.-U. (1993). *Geology of Bangladesh* (p. 160). Berlin: Borntraeger.

Renner, S. S. (2016). Available data point to a 4-km-high Tibetan Plateau by 40 Ma, but 100 molecular-clock papers have linked supposed recent uplift to young node ages. *Journal of Biogeography, 43*, 1479–1487.

Rowley, D. B., Pierrehumbert, R. T., & Currie, B. S. (2001). A new approach to stable isotope-based paleoaltimetry: Implications for paleoaltimetry and paleohypsometry of the high Himalaya since the Late Miocene. *Earth and Planetary Science Letters, 188*, 253–268.

Roy, R. K. (1968-69). *A note of the new clay deposits located in parts of the Sadar dn Sonamura sub-divison, Triprua, GSI Unpub*. Progress Report.

Roy, S. K., & Ghosh, P. K. (1979). On the occurrence of fossil woods of *Gluta* and *Anogeissus* in the Tertiary of Birbhum District, West Bengal, India. *Geophytology, 9*, 16–21.

Roy, S. K., & Ghosh, P. K. (1980). On the occurrence of *Palmoxylon coronatum* in West Bengal, India. *Ameghiniana, 17*(2), 130–134.

Roy, D. K., & Roser, B. P. (2013). Geochemical evolution of the Tertiary succession of the NW shelf, Bengal basin, Bangladesh: Implications for provenance, paleoweathering and Himalayan erosion. *Journal of Asian Earth Sciences, 78*, 248–262.

Roybarman, R. (1992). Geological history and hydrocarbon exploration in Bengal Basin. *Indian Journal of Geology, 64*(3), 235–238.

Sahni, A., & Mitra, H. C. (1980). Neogene palaeobiogeography of the Indian subcontinent with special reference to fossil vertebrates. *Palaeogeography, Palaeoclimatology, Palaeoecology, 31*, 39–62.

Salt, C. A., Alam, M. M., & Hossain, M. M. (1986). *Bengal Basin: current exploration of the hinge zone area of south – western Bangladesh* (pp. 55–57). Singapore: Proc. 6th offshore Southeast Asia (SEAPEX) Conference.

Saylor, J. E., Quade, J., Dettman, D. L., DeCelles, P. G., Kapp, P. A., & Ding, L. (2009). The late Miocene through present paleoelevation history of southwestern Tibet. *American Journal of Science., 309*, 1–42.

Schmitz, N., Verheyden, A., Beeckman, H., Kairo, J. G., & Koedam, N. (2006). Influence of a salinity gradient on the vessel characters of the mangrove species *Rhizophora mucronata*. *Annals of Botany, 98*, 1321–1330.

Ségalen, L., Lee-Thorp, J. A., & Cerling, T. (2007). Timing of C4 grass expansion across sub-Saharan Africa. *Journal of Human Evolution, 53*, 549–559.

Sen, I. (2006). *Xylotomical study of Neogene wood remains from different parts of Bengal Basin with remarks on palaeoenviroment*. Unpublished Thesis, Calcutta: Calcutta University.

Sen, I., & Bera, S. (2005). Petrified wood remains from the Neogene of Tripura, India. *Geophytology, 35*(1–2), 65–73.

Sen, I., Islam, M. S., & Bera, S. (2004). A fossil wood of *Cynometra* (Fabaceae) from the Plio-Pleistocene Dupi Tila Formation in Sylhet, Bangladesh. *Bangladesh Journal of Geology, 23*, 45–53.

Sen, I., Parua, D. K., Bera, S., Islam, S. U., & Poole, I. (2012). Contribution to the Neogene fossil wood records and palaeoecological understanding of Bangladesh. *Palaeontographica Abteilung B, 288*(1–4), 99–133. https://doi.org/10.1127/palb/288/2012/99.

Shackleton, N. J., Imbrie, J., & Pisias, N. G. (1988). The evolution of oceanic oxygen-isotope variability in the North Atlantic over the past three million years. *Philosophical Transactions of the Royal Society of London B, 318*, 679–686.

Spicer, R. A. (2017). Tibet, the Himalaya, Asian monsoons and Biodiversity – In what ways are they related? *Plant Diversity, 39*, 233–244.

Spicer, R. A., Su, T., Valdes, P. J., Farnsworth, A., Wu, F.-X., Shi, G., Spicer, T. E. V., & Zhou, Z.-K. (2020). Why the 'Uplift of the Tibetan Plateau' is a myth. *National Science Review, nwaa091*. https://doi.org/10.1093/nsr/nwaa091.

Srivastava, G., Paudayal, K. N., Utescher, T., & Mehrotra, R. C. (2018). Miocene vegetation shift and climate change: Evidence from the Siwalik of Nepal. *Global and Planetary Change, 161*, 108–120.

Su, T., Jacques, F. M. B., Spicer, R. A., Liu, Y.-S., Huang, Y.-J., Xing, Y.-W., & Zhou, Z.-K. (2013). Post-Pliocene establishment of the present monsoonal climate in SW China: Evidence from the late Pliocene Longmen megaflora. *Climate of the Past, 9*, 1911–1920.

Sun, X. J., & Wang, P. X. (2005). How old is the Asian monsoon system? Palaeobotanical records from China. *Palaeogeography Palaeoclimatology Palaeoecology, 222*, 181–222.

Sun, B.-N., Wu, J.-Y., Liu, Y.-S. C., Ding, S.-T., Li, X.-C., Xie, S.-P., Yan, D.-F., & Lin, Z.-C. (2011). Reconstructing Neogene vegetation and climates to infer tectonic uplift in western Yunnan, China. *Palaeogeography, Palaeoclimatology, Palaeoecology, 304*, 328–336.

Tang, H., Micheels, A., Eronen, J., & Fortelius, M. (2011). Regional climate model experiments to investigate the Asian monsoon in the Late Miocene. *Climate of the Past, 7*, 847–868.

Thayn, G. F., Tidwell, W. D., & Stokes, W. L. (1985). Flora of the Lower Cretaceous Cedar Mountain Formation of Utah and Colorado. Part III: *Icacinoxylon pittense* n. sp. *American Journal of Botany, 72*, 175–180.

Tiwari, R. P., Mehrotra, R. C., Srivastava, G., & Shukla, A. (2012). The vegetation and climate of a Neogene petrified wood forest of Mizoram, *India*. *Journal of Asian Earth Sciences, 61*, 143–165.

Uddin, A., & Lundberg, N. (1998). Cenozoic history of the Himalayan–Bengal system: Sand composition in the Bengal basin, Bangladesh. *Geological Society of America, Bulletin, 10*, 497–511.

Uddin, A., Kumar, P., Sharma, J. N., Syed, H., & A. (2007b). Heavy-mineral constraints on provenance of Cenozoic sediments from the foreland basins of Assam, India and Bangladesh: Erosional history of the eastern Himalayas and the Indo-Burman ranges. In M. A.

Mange & D. T. Wright (Eds.), *Heavy minerals in use: Developments in Sedimentology* 58, 823–847.

Uhl, D., Bruch, A. A., Traiser, C., & Klotz, S. (2006). Palaeoclimate estimates for the Middle Miocene Schrotzburg flora (S Germany): A multi-method approach. *International Journal of Earth Science, 95*, 1071–1085.

Utescher, T., & Mosbrugger, V. (2015). *The Palaeoflora Database*. www.palaeoflora.de.

Utescher, T., Bruch, A. A., Erdei, B., François, L., Ivanov, D., Jacques, F. M. B., Kern, A. K., Liu, Y.-S. (. C.)., & Mosbrugger, V. (2014). The Coexistence Approach—Theoretical background and practical considerations of using plant fossils for climate quantification. *Palaeogeo-graphy, Palaeoclimatology, Palaeoecology, 410*, 58–73.

Wan, S. M., Li, A. C., Clift, P. D., & Stuut, J. W. (2007). Development of the East Asian monsoon: Mineralogical and sedimentologic records in the northern South China Sea since 20 Ma. *Palaeogeography Palaeoclimatology Palaeoecology, 254*, 561–582.

Wang, B. (2006). *The Asian monsoon*. Berlin, Heidelberg: Springer Praxis Books, Springer.

Wang, P. X., Wang, B., Cheng, H., Fasullo, J., Guo, Z. T., Kiefer, T., & Liu, Z. Y. (2014). The global monsoon across timescales: Coherent variability of regional monsoons. *Climate of the Past, 10*, 2007–2052.

Wang, C. S., Dai, J., Zhao, X., Li, Y., Graham, S. A., He, D., Ran, B., & Meng, J. (2014). Outward-growth of the Tibetan Plateau during the Cenozoic: A review. *Tectonics, 621*, 1–43.

Wheeler, E. A., & Baas, P. (1991). A survey of the fossil record for dicotyledonous wood and its significance for evolutionary and ecological wood anatomy. *IAWA Bulletin New Series, 13*, 275–332.

Wheeler, E. A., & Baas, P. (1993). The potentials and limitations of dicotyledonous wood anatomy for climatic reconstructions. *Paleobiology, 19*, 487–498.

Wheeler, E. A., Pearson, R. G., La Pasha, C. A., Zack, T., & Hatley, W. (1986). Computer aided wood identification. *North Carolina Agricultural Research Service Bulletin, 474*, 1–96.

Wheeler, L. B., Galewsky, J., Herold, N., & Huber, M. (2016). Late Cenozoic surface uplift of the southern Sierra Nevada (California, USA): A paleoclimate perspective on lee-side stable isotope paleoaltimetry. *Geology, 44*(6), 451–454. https://doi.org/10.1130/G37718.1.

Wolfe, J. A., & Upchurch Jr., G. R. (1987). North American nonmarine climates and vegetation during the Late Cretaceous. *Palaeogeography, Palaeoclimatology, Palaeoecology, 61*, 33–77.

Woodcock, D. W., & Ignas, C. M. (1994). Prevalence of wood characters in eastern North America: What characters are most promising for interpreting climates from fossil wood. *American Journal of Botany, 81*, 1243–1251.

Xia, K., Tao, S., Liu, Y.-S. (. C.)., Xing, Y.-W., Jacques, F. M. B., & Zhou, Z.-K. (2009). Quantitative climate reconstructions of the late Miocene Xiaolongtan megaflora from Yunnan, Southwest China. *Palaeogeography, Palaeoclimatology, Palaeoecology, 276*, 80–86.

Xing, Y. W., Utescher, T., Jacques, F. M. B., Tao, S., Liu, Y. S., Huang, Y. J., & Zhou, Z.-K. (2012). Palaeoclimatic estimation reveals a weak winter monsoon in southwestern China during the late Miocene: Evidence from plant macrofossils. *Palaeogeography, Palaeoclimatology, Palaeoecology, 358-360*, 19–26.

Xu, J. X., Ferguson, D. K., Li, C. S., & Wang, Y. F. (2008). Late Miocene vegetation and climate of the Lühe region in Yunnan, southwestern China. *Review of Palaeobotany and Palynology, 148*, 36–59.

Yao, Y.-F., Bruch, A. A., Mosbrugger, V., & Li, C. S. (2011). Quantitative reconstruction of Miocene climate patterns and evolution in Southern China based on plant fossils. *Palaeogeography, Palaeoclimatology, Palaeoecology, 304*, 291–307.

Yao, Y.-F., Bruch, A. A., Cheng, Y.-M., Mosbrugger, V., Wang, Y.-F., & Li, C.-S. (2012). Monsoon versus uplift in southwestern China–Late Pliocene climate in Yuanmou Basin, Yunnan. *PLOS One, 7*, e37760. https://doi.org/10.1371/journal.pone.0037760.

Zachos, J., Pagani, M., Sloan, L., Thomas, E., & Billups, K. (2001). Trends, rhythms, and aberrations in global climate 65 Ma to present. *Science, 292*, 686–693.

Zheng, H. B., Powell, C. M. A., Read, D. K., Wang, J. L., & Wang, P. X. (2004). Late Miocene and mid-Pliocene enhancement of the East Asian monsoon as viewed from the land and sea. *Global and Planetary Change, 41*, 147–155.